Article

Cell Reports

Activated CD8$^+$ T Cells Cause Long-Term Neurological Impairment after Traumatic Brain Injury in Mice

Graphical Abstract

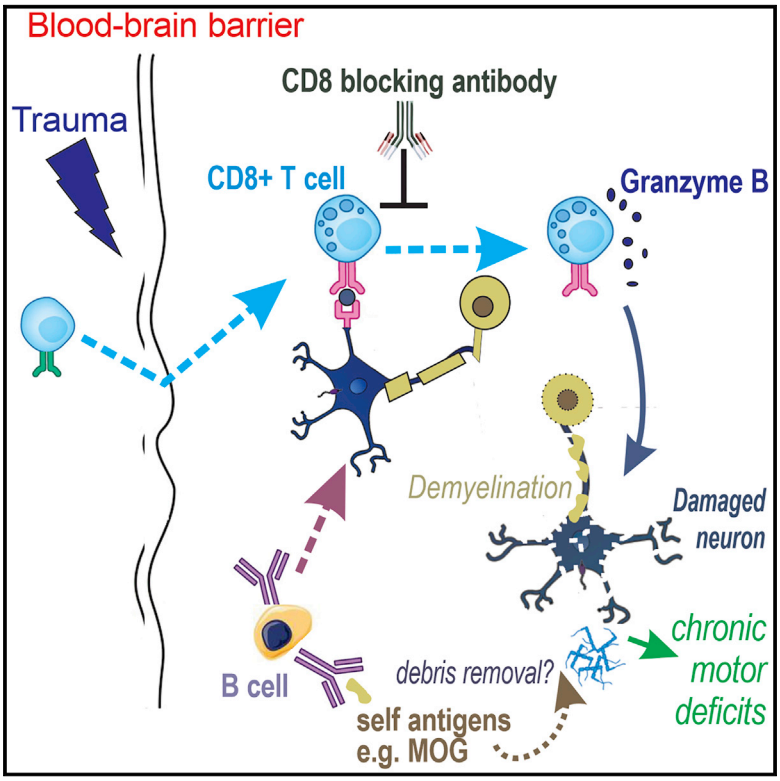

Highlights

- Granzyme B$^+$ CD8$^+$ T cells accumulate in the brain after traumatic brain injury (TBI)
- Brain CD8$^+$ T cells contribute to chronic motor deficits and myelin pathology
- Deficiency/depletion of CD8$^+$ T cells promotes neurological recovery following TBI
- B cells and autoreactive antibodies appear to play a regulatory role in TBI

Authors

Maria Daglas, Dominik F. Draxler, Heidi Ho, ..., Frank Alderuccio, Maithili Sashindranath, Robert L. Medcalf

Correspondence

maithili.sashindranath@monash.edu (M.S.), robert.medcalf@monash.edu (R.L.M.)

In Brief

Daglas et al. show that granzyme B$^+$CD8$^+$ T cells accumulate in the brain after traumatic brain injury, triggering chronic neurological/motor impairment and myelin pathology. Genetic deficiency/pharmacological depletion of CD8$^+$ T cells, but not B cells, promotes recovery post-injury and offers a therapeutic option to minimize long-term disabilities in trauma patients.

Daglas et al., 2019, Cell Reports *29*, 1178–1191
October 29, 2019
https://doi.org/10.1016/j.celrep.2019.09.046

CellPress

OPEN ACCESS
CellPress

Cell Reports
Article

Activated CD8$^+$ T Cells Cause Long-Term Neurological Impairment after Traumatic Brain Injury in Mice

Maria Daglas,[1] Dominik F. Draxler,[1] Heidi Ho,[1] Fiona McCutcheon,[1] Adam Galle,[1] Amanda E. Au,[1] Pia Larsson,[1] Julia Gregory,[1] Frank Alderuccio,[2] Maithili Sashindranath,[1,3,*] and Robert L. Medcalf[1,3,4,*]

[1]Molecular Neurotrauma and Haemostasis, Australian Centre for Blood Diseases, Central Clinical School, Monash University, Melbourne, VIC 3004, Australia

[2]Department of Immunology and Pathology, Central Clinical School, Monash University, Melbourne, VIC 3004, Australia

[3]Senior author

[4]Lead Contact

*Correspondence: maithili.sashindranath@monash.edu (M.S.), robert.medcalf@monash.edu (R.L.M.)

https://doi.org/10.1016/j.celrep.2019.09.046

SUMMARY

Traumatic brain injury (TBI) leaves many survivors with long-term disabilities. A prolonged immune response in the brain may cause neurodegeneration, resulting in chronic neurological disturbances. In this study, using a TBI mouse model, we correlate changes in the local immune response with neurodegeneration/neurological dysfunction over an 8-month period. Flow cytometric analysis reveals a protracted increase in effector/memory CD8$^+$ T cells (expressing granzyme B) in the injured brain. This precedes interleukin-17$^+$CD4$^+$ T cell infiltration and is associated with progressive neurological/motor impairment, increased circulating brain-specific autoantibodies, and myelin-related pathology. Genetic deficiency or pharmacological depletion of CD8$^+$ T cells, but not depletion of CD4$^+$ T cells, improves neurological outcomes and produces a neuroprotective Th2/Th17 immunological shift, indicating a persistent detrimental role for cytotoxic T cells post-TBI. B cell deficiency results in severe neurological dysfunction and a heightened immune reaction. Targeting these adaptive immune cells offers a promising approach to improve recovery following TBI.

INTRODUCTION

Traumatic brain injury (TBI) following a physical impact to the head causes a cascade of neuroinflammatory and pathophysiological events, resulting in long-lasting physical and cognitive disabilities. According to the World Health Organization, TBI will become the third major global cause of mortality and disability by 2020 (Maas et al., 2008). Aside from the well-recognized progressive cognitive ailments that can accompany TBI, sensorimotor deficits are a major complaint of TBI patients but receive little attention in the research setting (Walker and Pickett, 2007).

Neuroinflammation plays an important role in tissue repair and preventing infection early after injury. However, prolonged immune activation has been thought to cause further brain damage and impede recovery (Plesnila, 2016). Previous TBI-related studies have mainly focused on short-term inflammatory responses, typically involving innate immune cells (Jassam et al., 2017; Plesnila, 2016). However, adaptive immune cells can accumulate in the lesion and persist for months after CNS injury (Ankeny et al., 2006; Beck et al., 2010). This accumulation has been regarded as deleterious, given that the absence of T and/or B cells conferred protection following stroke or spinal cord injury (SCI) (Ankeny et al., 2009; Hurn et al., 2007; Wu et al., 2012). However, *Rag1*$^{-/-}$ mice (devoid of mature T and B cells) failed to show neuroprotection within 1 week after TBI (Weckbach et al., 2012), although later time points were not investigated. Genetic deficiency of CD8$^+$ or CD4$^+$ T cell subsets, but not B cells, was also shown to improve infarct size and neurological deficits 1 day after ischemic stroke (Yilmaz et al., 2006). Specific subtypes of CD4$^+$ T helper (Th) cells can have contrasting effects after injury: Th1 and Th17 responses exaggerate inflammation and drive autoimmunity, whereas a Th2 response attenuates inflammation and can be protective (Dardiotis et al., 2012).

The disruption of the blood-brain barrier (BBB) following TBI can result in the exposure of brain-derived antigens, including myelin, which can promote the activation of autoreactive cells and potentially lead to a pathogenic autoimmune response (Dardiotis et al., 2012). Autoreactive antibodies/lymphocytes specific to CNS antigens, including myelin basic protein, glial fibrillary acidic protein, and S100B, are increased in the cerebrospinal fluid (CSF) and/or serum of TBI patients (Raad et al., 2014). The association of adaptive immunity and autoimmunity in the brain following TBI over the long term is not clear.

Many epidemiological studies have described a link between TBI and late-stage neurodegeneration (Bazarian et al., 2009; Sundman et al., 2014), while only a few have investigated the immune response in the promotion of chronic injury (Bramlett and Dietrich, 2015). This is an important area of research that is missing in the TBI-related literature. Hence, the present study investigated the role of the adaptive immune response with long-term neurological deficiency after TBI over an extended

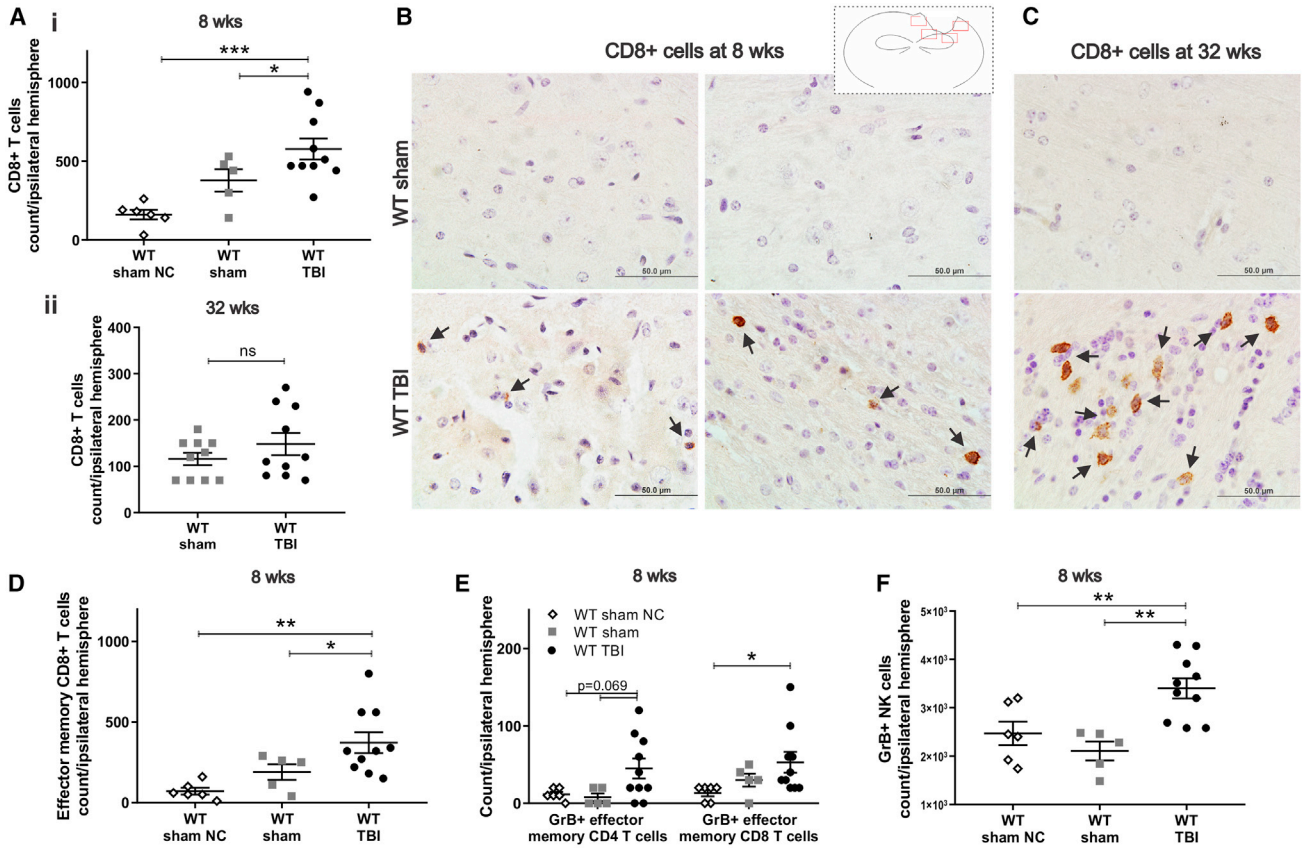

Figure 1. Effector Memory CD8$^+$ T Cells Are Increased in the Ipsilateral Brain and Express Granzyme B (in Addition to NK Cells) at 8 Weeks following TBI

(A) Flow cytometric analysis revealed significant increases in total counts of CD8$^+$ T cells at (i) 8 weeks but not (ii) 32 weeks (trending) in the ipsilateral hemisphere of WT TBI mice, compared to sham and/or sham NC mice.

(B and C) Representative immunostained images (×1,000 magnification, scale bar, 50 μm) of CD8$^+$ cells present at the injured site at (B) 8 and (C) 32 weeks post-TBI compared to sham control. The schematic of the brain shows regions of interest (red outlined boxes).

(D) Flow cytometry showed an increase in effector memory CD8$^+$ T cells in the ipsilateral hemisphere of WT mice at 8 weeks post-TBI compared to sham and sham NC mice.

(E and F) Flow cytometry analysis detected a significant increase in GrB$^+$ expression in (E) CD8$^+$ T cells but not CD4$^+$ T cells (trending increase: $p = 0.069$) between TBI and sham NC mice.

(F) GrB$^+$ expression in NK cells is increased at 8 weeks post-TBI compared to sham/sham NC controls.

*$p < 0.05$, **$p < 0.01$, and ***$p < 0.001$. One-way ANOVA with Newman-Keuls post hoc test ($n = 10$ biological replicates for TBI, $n = 5$ biological replicates for sham, and $n = 6$ biological replicates for sham NC mice; for Ai and D–F). Unpaired two-tailed t test between TBI ($n = 10$ biological replicates) and sham ($n = 10$ biological replicates) for 32 weeks (Aii) from one independent experiment. Error bars represent SEMs.

See also Figures S1, S2, and S3.

(32 weeks) period, using genetic approaches and pharmacological depletion techniques.

RESULTS

A Persistent Adaptive Immune Response Occurs in Mice following TBI

Flow cytometric analyses revealed a significant increase in CD8$^+$ T cells in the ipsilateral brain at 8 weeks post-TBI compared to sham controls without craniotomy (sham NC) and sham mice (i.e., with craniotomy) (Figure 1Ai). Note that these findings were confirmed in additional independent experiments at the 8-week time point at which we also observed an increase in both CD8$^+$ T cells and effector memory CD8$^+$ T cells (Figures S1A and S1B). Although a trending (yet not significant) increase in CD8$^+$ T cell counts was seen in the ipsilateral brain at 32 weeks post-TBI (Figure 1Aii), the proportion of CD8$^+$ T cells (of all T cells) were significantly increased at both 8 and 32 weeks post-TBI (Figures S2Ai, S2Aii, and S2Ei). Histological analysis confirmed the presence of immune cells at the injured site at 8 and 32 weeks post-TBI (Figures S3A and S3B). Immunostaining revealed the localization of CD8$^+$ T cells around the lesion at the 8-week time point (Figure 1B) and at 32 weeks post-TBI (Figure 1C).

Effector memory CD8$^+$ T cells were increased in the ipsilateral brain at 8 weeks post-TBI compared to sham NC controls and/or sham mice (Figure 1D). Granzyme B expression (GrB$^+$) was

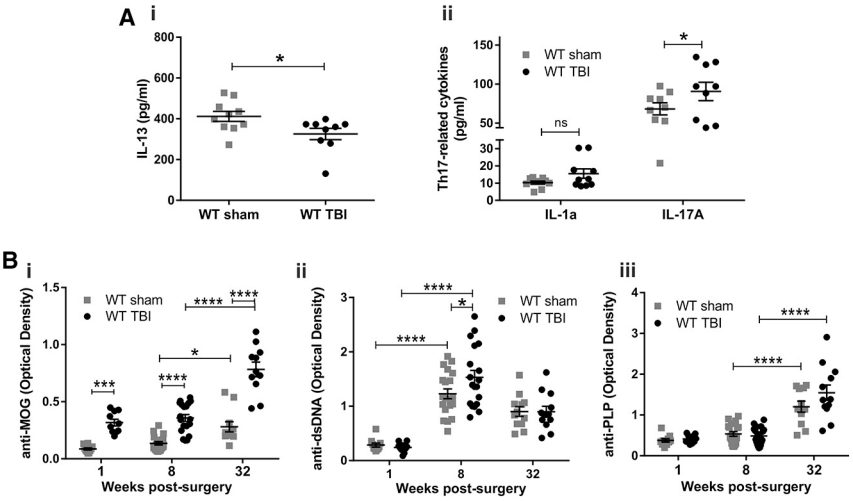

Figure 2. Prominent Th17-type Response and Increased Autoreactivity in the Circulation of WT Mice after TBI

(A) Multiplex serum cytokine analysis at 8 weeks after TBI showed (i) a reduction in anti-inflammatory cytokine IL-13. *$p < 0.05$. Unpaired two-tailed t test between TBI (n = 9–10 biological replicates) and sham (n = 10 biological replicates) mice. (ii) In contrast, an increase was seen in the Th17-related pro-inflammatory cytokine IL-17A, but no change in IL-1α in TBI mice compared to sham controls. *$p < 0.05$. Two-way ANOVA; Newman-Keuls post hoc correction for multiple comparisons. Note that the 32-week time point was not assessed. Error bars represent SEMs.

(B) Increase in circulating autoantibodies against (i) MOG, (ii) dsDNA, but not (iii) PLP over the course of 32 weeks post-TBI compared to sham controls, measured by ELISA.

*$p < 0.05$, ***$p < 0.001$, and ****$p < 0.0001$. Two-way ANOVA; Bonferroni post hoc test (n = 10–20 biological replicates/group, 2 technical replicates, from 2 independent experiments). Error bars represent SEMs. See also Figure S4.

increased in these effector memory $CD8^+$ T cells and natural killer (NK) cells and only trending (not significant) in effector memory $CD4^+$ T cells at 8 weeks post-TBI (Figures 1E and 1F). Similar trends are seen in proportions of these immune populations in the injured brain (Figures S2Aiii–S2Av and S2Eii). There were no changes in Fas ligand (FasL) expressing $CD8^+$ T cells (or other T cells/NK cells) between TBI and sham controls (not shown). These data are consistent with the idea that $CD8^+$ T cells are mediating damage via the granzyme/perforin pathway, rather than through the apoptotic pathway.

$CD4^+$ T cells were not significantly increased at 8 and 32 weeks post-TBI (Figures S1Ci and S1Cii), although an increase in $CD69^+$ activated B cells at the 8 week time point was seen (Figure S1D). NKT-like cells or inflammatory populations (monocytes and $CD11b^+$ conventional dendritic cells [DCs]) were not altered between TBI and sham controls at 8 weeks (Figures S1E and S1F) and 32 weeks (not shown). Similar trends are seen in the proportions of these immune populations in the injured brain (Figures S2Eiii–S2Evii). As expected, contralateral hemispheres of injured and sham mice displayed a normal cellular immune profile (data not shown). That no changes of any immune marker described above between TBI and sham-operated mice were observed in the cervical lymph nodes (cLNs) (not shown) indicates that TBI causes a more localized cellular immune response in the brain at the later time points.

A Th17-like Response Is Evident in the Circulation and Injured Brain following TBI

Serum levels of the anti-inflammatory cytokine interleukin-13 (IL-13) were significantly reduced in wild-type (WT) mice at 8 weeks post-TBI (Figure 2Ai). In contrast, levels of IL-17A, a pro-inflammatory Th17-related cytokine, was elevated as well as a non-significant increase in IL-1α, after injury (Figure 2Aii). There were no significant changes in the remaining 19 cytokines/chemokines analyzed. To further confirm that TBI induces a Th17 response, we studied the cytokine response in brain-derived lymphocytes stimulated with phorbol 12-myristate 13-acetate (PMA)/ionomycin *ex vivo*. We show that IL-17-producing $CD4^+$ T cells and interferon-γ (IFN-γ)-producing $CD4^+$ T cells are specifically elevated in the ipsilateral cortex at 1 week after TBI (Figure S4).

Circulating Autoantibodies against Myelin and dsDNA Are Generated following TBI

Circulating autoantibodies to all three antigens (myelin oligodendrocyte glycoprotein [MOG], proteolipid protein [PLP], and double-stranded DNA [dsDNA]) were detected post-TBI in a temporally distinct manner (Figures 2Bi–2Biii). Anti-MOG antibodies were significantly increased relative to sham controls at the 1-, 8-, and 32-week time points. In contrast, anti-PLP antibodies were present only at the 32-week time point in both sham and injured mice. Anti-dsDNA antibodies were markedly elevated at 8 weeks in sham controls and further increased following TBI; they were still elevated at 32 weeks in both sham and injured mice. These data indicate that TBI results in an autoantibody response. The observation that autoantibodies also occur in sham mice likely indicates that the craniotomy procedure is causing a mild TBI, as previously described (Sashindranath et al., 2015). Total serum immunoglobulin G (IgG) levels remain unchanged between TBI and sham controls at 8 and 32 weeks post-surgery (data not shown), confirming that this increase in autoantibodies detected after TBI was specific. However, an age-related increase in serum IgG was also observed, as reported in humans (Gonzalez-Quintela et al., 2008; Jazayeri et al., 2013), and this may therefore be reflected in the elevated autoantibody response seen between 8 and 32 weeks.

Mice Deficient in B Cells Show a Heightened Immune Response following TBI

We next investigated the role of B cells and their derived antibodies in TBI by studying B cell-deficient μ-MT mice. In contrast to WT mice (Figure S1F), inflammatory cells, including monocytes and $CD11b^+$ cDC, were significantly elevated at 8 weeks post-TBI in the ipsilateral cortex of μ-MT mice (Figure 3Ai), suggesting

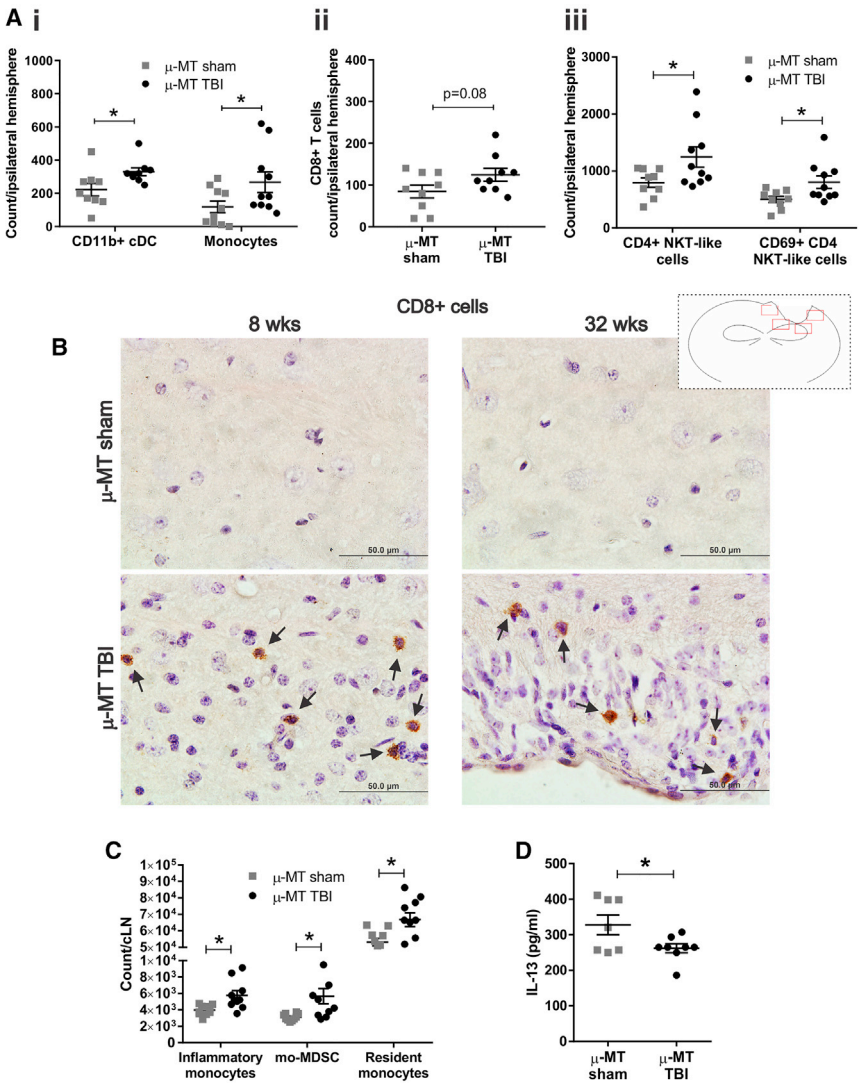

Figure 3. Mice Deficient in B Cells (μ-MT) Have a Heightened Immune Response in the Brain and Periphery at 8 Weeks after TBI

(A) Flow cytometry analysis of the brain showing an increase in total counts of (i) inflammatory cells (monocytes and CD11b$^+$ cDCs), (ii) CD8$^+$ T cells (trending $p = 0.08$), and (iii) CD4$^+$ NKT-like cells and CD69-activated CD4$^+$ NKT-like cells at 8 weeks post-TBI compared to sham in μ-MT mice (n = 9–10 biological replicates/group).

(B) Representative immunostained brain sections (×1,000 magnification, scale bar, 50 μm) of CD8 staining in the lesion at 8 and 32 weeks post-TBI, compared to sham control. The schematic of the brain shows regions of interest (red outlined boxes).

(C) Various monocyte subtypes were elevated in injured μ-MT mice in the cervical lymph node (n = 10 biological replicates/group), detected by flow cytometry.

(D) Multiplex plasma cytokine analysis revealed reduced circulating anti-inflammatory IL-13 cytokine levels at 8 weeks after TBI (n = 8 biological replicates) compared to sham mice (n = 7 biological replicates).

*$p < 0.05$, **$p < 0.01$, and ***$p < 0.001$. Unpaired two-tailed t test. One independent experiment. Error bars represent SEMs.

See also Figures S2 and S3.

a role for B cells in attenuating inflammation. We found a trending increase ($p = 0.08$) in total CD8$^+$ T cell counts in the injured brains of μ-MT mice at this time point (Figure 3Aii). A 2-fold significant increase in the proportion of CD8$^+$ T cells was also seen (Figure S2Bii). This was similar to that observed in WT mice, suggesting that the CD8$^+$ T cell response following TBI is B cell independent. CD4$^+$ NKT-like cells and CD69 activated CD4$^+$ NKT-like cells were also elevated in the injured brains of these mice (Figure 3Aiii). As this was not seen in the WT cohort at 8 weeks post-TBI (Figure S1E), it appears that the absence of B cells promotes a directed T cell response to injury. A similar trend was observed in the proportions of the mentioned immune populations in the injured brains of μ-MT mice (Figures S2Bi–S2Biv).

Immunohistochemical staining confirmed that immune cells (Figure S3C), specifically CD8$^+$ cells, were present in the lesion at 8 weeks (Figure 3B) and at 32 weeks (not shown).

μ-MT mice were also found to have an active systemic immune response at the 8-week time point post-TBI. Resident and inflammatory monocytes, as well as monocyte-like myeloid-derived suppressor cells (mo-MDSCs), were significantly increased in the cLNs of μ-MT mice even at this chronic phase of TBI (Figure 3C). Hence, μ-MT mice have a more pronounced immune response involving both innate and adaptive immune cells at 8 weeks following TBI compared to WT mice.

Plasma levels of the anti-inflammatory cytokine IL-13 were reduced in injured μ-MT mice (Figure 3D) as seen in WT mice (Figure 2Ai), suggesting that the T cell-directed response rather than the B cell-directed response in these mice correlates with the suppression of IL-13 cytokine activity.

Genetic Deletion of CD8$^+$ T Cells Does Not Result in a Heightened Immune Response after TBI

β-2-microglobulin-deficient (β2m$^{-/-}$) mice were used to characterize the role of CD8$^+$ T cells in TBI. These mice were assessed up to 8 weeks after injury but not up to 32 weeks post-TBI due to the limited number of mice available. Remarkably, no major changes in inflammatory cells, NKT-like cells, or B cells were observed between β2m$^{-/-}$ TBI and sham animals at 8 weeks, indicating relatively normal immune functioning within the injured brain and draining cLNs (data not shown). We did, however, observe a significant increase in effector memory CD4$^+$ T cells in the injured brains of β2m$^{-/-}$ mice (Figure 4A) and the proportion of effector memory cells of CD4$^+$ T cells (Figure S2C). The presence of immune cells (likely CD4$^+$ T cells) in the lesioned area was also confirmed histologically (Figure S3D).

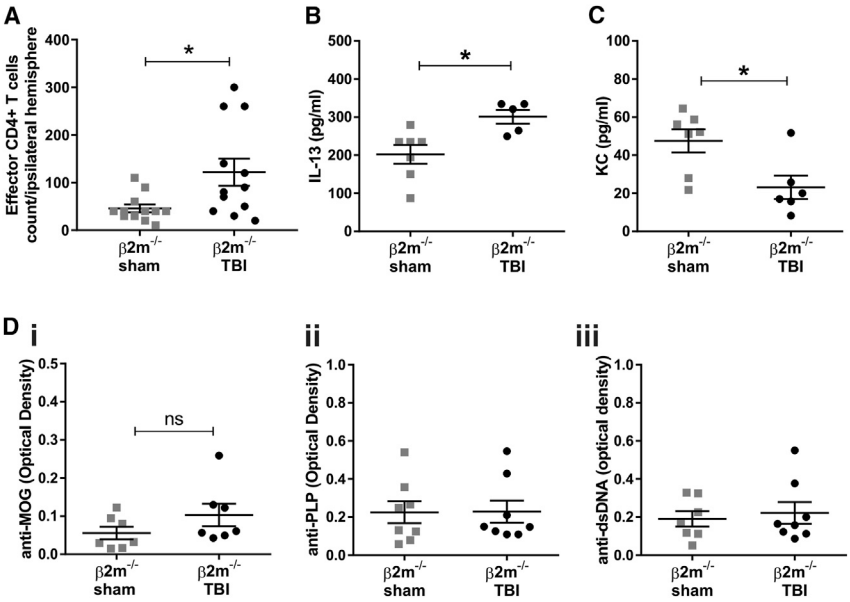

Figure 4. CD8 T Cell-Deficient Mice ($\beta2m^{-/-}$) Display Diminished Immune Activity and an Anti-inflammatory Response in the Brain and Periphery at 8 Weeks Post-TBI

(A) Flow cytometric analysis of the brain showing an increase in effector memory $CD4^+$ T cells in $\beta2m^{-/-}$ mice (n = 12 biological replicates/group from 3 independent experiments) after TBI.

(B and C) Multiplex serum cytokine analysis shows that circulating (B) anti-inflammatory cytokine IL-13 is increased, whereas (C) pro-inflammatory keratinocyte chemoattractant (KC) is decreased in $\beta2m^{-/-}$ mice after TBI (n = 5–6 biological replicates) relative to sham control (n = 7 biological replicates).

(D) No changes in circulating (i–iii) autoreactive antibodies between TBI and sham $\beta2m^{-/-}$ animals (n = 7–8 biological replicates/group), measured by ELISA.

*$p < 0.05$. Unpaired two-tailed t test. Error bars represent SEMs.

See also Figures S2 and S3.

There were no significant changes in serum anti-MOG, PLP, or dsDNA antibody levels (Figures 4Di–4Diii) in $\beta2m^{-/-}$ mice following TBI. The low baseline autoantibody titers detected in $\beta2m^{-/-}$ mice are likely to be related to β2m/major histocompatibility complex class I (MHC class I) involvement in antibody responses, as $\beta2m^{-/-}$ mice have an abnormally reduced IgG half-life (Christianson et al., 1997). However, there was a 50% increase in IL-13 (Figure 4B), a classic Th2-related cytokine. This was not seen in WT and μ-MT mice (Figures 2Ai and 3D). A 2-fold reduction in the plasma levels of the pro-inflammatory KC (keratinocyte chemoattractant) was also seen in these mice after trauma (Figure 4C). Hence, the absence of a $CD8^+$ T cell response coincided with an increase in anti-inflammatory Th2-related cytokine IL-13 in the injured mice that may be beneficial after injury.

Prolonged Neurological Deterioration in WT and μ-MT Mice but Not $\beta2m^{-/-}$ Mice after TBI

We next evaluated neurological changes in WT, $\beta2m^{-/-}$, and μ-MT mice over the long term (i.e., up to 32 weeks) post-TBI. We observed previously unreported neurological changes that became apparent from 3–4 weeks post-TBI (including tail spasms, tail weakness, and uneven gait; Video S1) and peaked at 25–32 weeks (Figure 5A). As seen in Figure 5A, μ-MT mice also experienced progressive neurological impairment over the course of 32 weeks. However, the neurological deficits in μ-MT mice were similar to the WT mice but attained maximal neurological impairment approximately 12 weeks earlier than the WT TBI cohort. $\beta2m^{-/-}$ mice exhibited significantly fewer and less frequent behavioral abnormalities evaluated over 8 weeks post-TBI (Figure 5B), further supporting a damaging role for $CD8^+$ T cells.

$\beta2m^{-/-}$ Mice Do Not Display Gait Deficits following TBI

Changes in motor function following TBI was qualitatively evaluated using the DigiGait apparatus. WT and μ-MT mice experienced gait impairment of the right forelimb (Figures 5Ci and 5Cii) and right hindlimb (Figures 5Di and 5Dii) that continued to deteriorate over 32 weeks post-TBI. A progressive increase in swing duration suggesting weakness or "dragging" was noticed in the right hindlimb of injured WT mice (Figure 5Di). In addition, injured WT mice showed an increase in the duration of propulsion in the right forelimb, which was possibly a compensatory mechanism due to right hindlimb weakness (Figure 5Ci). Propulsion duration was also significantly affected in both right limbs of μ-MT mice over the 32-week period, particularly between 12 and 18 weeks after injury (Figures 5Cii and 5Dii), similar to that seen in Figure 5A. Sham WT and sham μ-MT mice also displayed a progressive trend on the DigiGait over the 32 weeks, which is consistent with our report that the craniotomy procedure promotes a mild brain injury (Sashindranath et al., 2015).

No major differences in gait were seen between $\beta2m^{-/-}$ injured and sham-operated mice (Figures 5Ciii and 5Diii), which corroborates the absence of any significant changes in neurological score in these mice following TBI (Figure 5B). These results complement the cumulative neurological scoring data in Figures 5A and 5B and confirm that TBI induces prolonged motor function abnormalities in a process that is dependent on the presence of $CD8^+$ T cells.

Pharmacological Depletion of $CD8^+$ T Cells Leads to Improved Outcomes following TBI

C57BL/6 mice were depleted of $CD8^+$ T cells beginning at the 4-week time point after TBI. This time was selected to precede the increase in $CD8^+$ T cells seen in WT mice (Figure 1Ai). We were not able to deplete mice of $CD8^+$ T cells (or $CD4^+$ T cells) for longer periods past 8 weeks (e.g., 32 weeks) due to ethical regulations. Flow cytometric analysis of blood confirmed the depletion of the $CD8^+$ T cells compared to isotype control (>98% depletion on day 6; Figure 6A). $CD8^+$ T cell-depleted

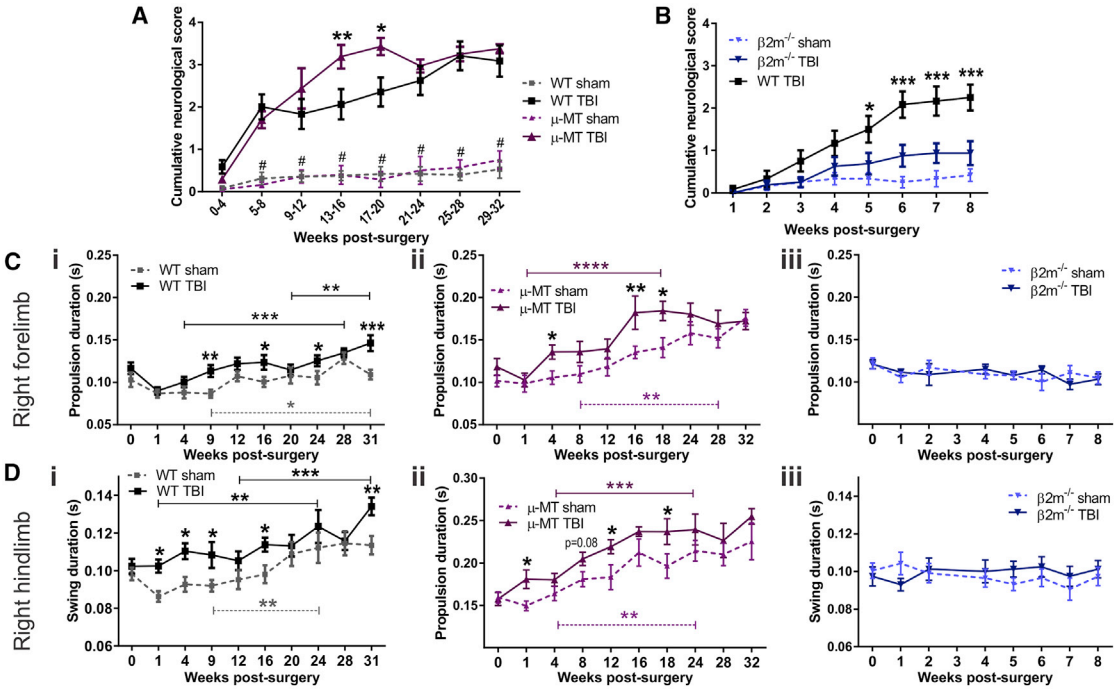

Figure 5. Severe Neurological Dysfunction Observed in WT and μ-MT Mice, Whereas CD8⁺ T Cell-Deficient β2m$^{-/-}$ Mice Are Protected after TBI

(A) Significant neurological deficits are seen up to 32 weeks in injured WT mice (n = 12 biological replicates/group). See also Video S1. μ-MT mice display an earlier and more severe neurological impairment between 12 and 20 weeks after TBI (n = 8–24 biological replicates), compared to WT mice. Sham-operated controls (n = 7–23 biological replicates for μ-MT) show only mild neurological deficits in both cohorts. Note: statistical analysis compared all groups, although the significance shown (*) is between WT TBI and μ-MT TBI. # represents the significance ($p < 0.0001$) between WT TBI versus WT sham and μ-MT TBI versus μ-MT sham mice. *$p < 0.05$ and **$p < 0.01$. Two-way ANOVA; Bonferroni post hoc test. Error bars represent SEMs.

(B) β2m$^{-/-}$ mice have significantly improved neurological outcomes compared to WT (n = 12 biological replicates) over 8 weeks after TBI (n = 16 biological replicates), with no significant changes compared to sham (n = 12 biological replicates). Note: statistical analysis compared β2m$^{-/-}$ TBI to WT TBI and β2m$^{-/-}$ sham groups, in which the significance shown (*) is between β2m$^{-/-}$ TBI and WT TBI. These WT mice are the same cohort as presented in (A), but analyzed weekly over this 8-week period. *$p < 0.05$ and ***$p < 0.001$. Two-way ANOVA; Bonferroni post hoc test. Error bars represent SEMs.

(C and D) DigiGait analysis revealed a progressive gait impairment of the (C) right forelimb and (D) right hindlimb in (i) WT mice (n = 12 biological replicates/group) and (ii) μ-MT mice (TBI, n = 6–11 biological replicates; sham, n = 6–10 biological replicates) during the 32-week period, but not in (iii) β2m$^{-/-}$ mice (n = 8–12 biological replicates/group) over 8 weeks, after TBI.

*$p < 0.05$, **$p < 0.01$, ***$p < 0.001$, and ****$p < 0.0001$. Two-way ANOVA; Fisher's least significant difference (LSD) test. Error bars represent SEMs.

mice showed an improved neurological outcome compared to control mice from the time of injection at 4 weeks to 8 weeks post-TBI (Figure 6B), further supporting a deleterious role for CD8⁺ T cells during the chronic phase of TBI.

Flow cytometric analysis of the injured brain revealed no change in the CD4⁺ T cell population, but an increase in effector memory CD4⁺ T cells (within the CD4⁺ T cell population) in CD8⁺ T cell-depleted mice (Figures 6Ci and 6Cii). These results are consistent with those from the β2m$^{-/-}$ mice, which also showed an increase in effector memory CD4⁺ T cells and reduced neurological deficit at 8 weeks post-injury. A similar trend was observed in the proportion of these lymphocytes in the injured brains of CD8 depleted mice at the same time point (Figure S2D). It is important to note that these increased CD4⁺ T cells in the brains of CD8⁺ T cell-depleted mice (again confirmed in an additional independent experiment; Figure S5B) were not found to be increased regulatory T cells (Tregs) (Figures S5Ai and S5Aii). We also found an increase ($p = 0.06$) in Th2-related cytokine IL-4 in CD8⁺ T cell-depleted mice relative to IgG2b isotype control at 8 weeks post-TBI (Figure 6Di). A 2-fold increase in monocyte chemoattractant protein-1 (MCP-1) and a 66% decrease in pro-inflammatory (neutrophil attracting) KC chemokine in anti-CD8 antibody-injected mice (Figures 6Dii and 6Diii) were also observed, further supporting the Th2/Th17 shift away from a systemic inflammatory environment.

CD8⁺ T cell-depleted mice were also evaluated for circulating autoantibodies at 8 weeks post-TBI. As shown in Figures 6Ei–6Eiii, antibodies against MOG, PLP, and dsDNA were significantly elevated in CD8⁺ T cell-depleted mice compared to injured isotype control mice. Since these autoantibodies are increased in the CD8 depleted mice that were protected from TBI, this suggests that they may even be protective rather than detrimental.

Assessment of cognitive function at 7–8 weeks post-TBI using the Morris water maze (MWM) showed no changes, suggesting that the protective effect of CD8⁺ depletion is restricted to motor function (Figures S6A and S6B).

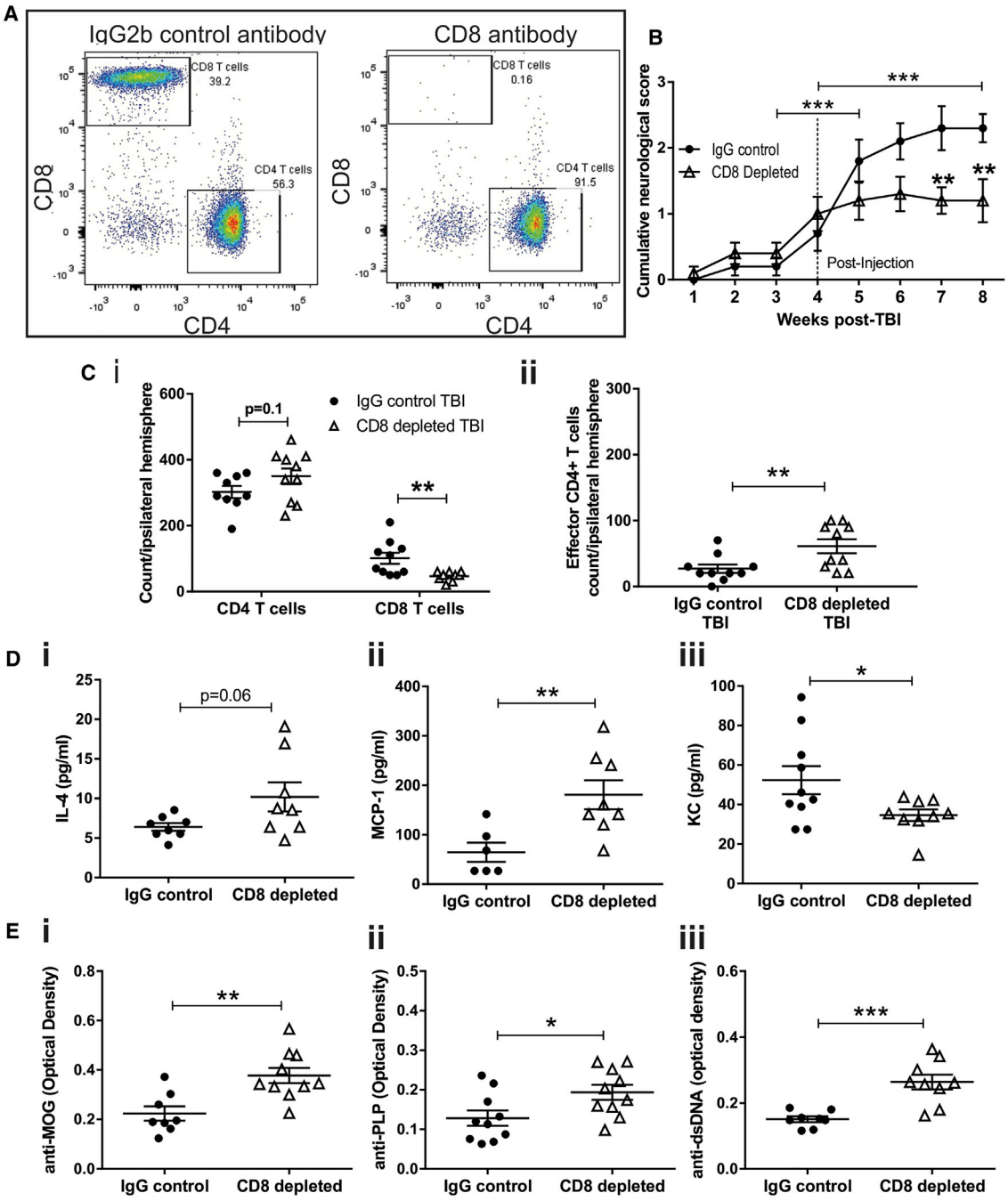

Figure 6. Depleting Mice of CD8$^+$ T Cells at the Chronic Phase of TBI Leads to Improved Neurological Deficits, a Th2-type Immune Response, and Increased Autoreactivity over an 8-Week Period

(A) Confirmed depletion of CD8$^+$ T cells with the CD8 neutralizing antibody compared to IgG2b isotype control at day 6 post-injection (>98% depleted) by flow cytometry. This plot is representative of n = 10 biological replicates/group.

(B) CD8 depleted mice (n = 10 biological replicates/group) have improved neurological outcomes compared to isotype control mice, from the time of injection at 4 weeks to 8 weeks post-TBI. **p < 0.01 and ***p < 0.001. Two-way ANOVA; Bonferroni post hoc test. Error bars represent SEM.

(C) Flow cytometric analysis shows a significant reduction in absolute counts of (i) CD8$^+$ T cells, but not CD4$^+$ T cells, in the injured brains of CD8 depleted mice compared to IgG2b control (n = 9–10 biological replicates/group), although there has been some recovery of CD8$^+$ T cells by 8 weeks in the depleted group. (ii) Increased counts of effector memory CD4$^+$ T cells in the injured brains of CD8 depleted mice were seen compared to IgG2b control at 8 weeks post-TBI (n = 10 biological replicates/group).

(legend continued on next page)

Behavioral Changes Are Not Detected in Injured Mice Depleted of CD4$^+$ Cells

Since there was an increase in effector memory CD4$^+$ T cells in the ipsilateral cortex in both CD8$^+$ T cell-deficient and -depleted mice, we sought to determine the potential contribution of CD4$^+$ T cells during the chronic phase post-TBI. CD4 depleted mice were subjected to the MWM to gauge cognition (Figures S6A and S6B), and to neurological (Figure S6C) and DigiGait testing (Figures S6Di and S6Dii). CD4$^+$ T cell depletion resulted in no discernible change to the neurological score, nor to motor or cognitive function (although there was a trend for improvement in MWM) (Figures S6A–S6D).

Successful depletion of CD4$^+$ T cells in both the blood and cLNs (Figure S6E) was confirmed by flow cytometry. CD4$^+$ T cells were significantly decreased in the injured brain, as expected in CD4 depleted mice (Figure S6F). A compensatory increase in CD8$^+$ T cells (Figure S6G) but not effector memory CD8$^+$ T cells (Figure S6H) was seen in these mice. GrB expression in the CD8$^+$ T cell population was also unchanged in CD4 depleted mice following TBI (Figure S6I).

Myelin Vacuolization in the Spinal Cords of WT and μ-MT Mice, but Not in the Absence of a CD8 T Cell Response Post-TBI

Because of the strong inflammatory response seen after TBI and also the multiple sclerosis (MS)-like neurobehavioral/autoantibody changes (e.g., tail and hindlimb weakness), we investigated myelin pathology in spinal cord sections of WT, μ-MT, β2m$^{-/-}$, and CD8$^+$ T cell-depleted mice stained at 8 or 32 weeks post-TBI, using luxol fast blue (LFB) stain (Figures 7A and 7B). No extensive demyelination was evident within the spinal cords of any mouse genotype at either time point post-TBI as LFB staining was evenly distributed. However, WT mice showed a significant increase in myelin vacuolization (reduced density of packing in the myelin layers) in the thoracic/lumbar spinal cord at 8 weeks post-TBI and an increased (yet non-significant) trend at 32 weeks (Figure 7Bi). In contrast, the μ-MT mice did not display any increase in vacuolization at 8 weeks, but it was markedly increased at 32 weeks (Figure 7Bii). β2m$^{-/-}$ mice also showed no increase in myelin vacuolization (Figure 7Biii), and CD8$^+$ T cell-depleted mice showed a significant reduction in vacuolization compared to isotype controls at 8 weeks post-TBI (Figure 7Biv), consistent with improved neurological outcomes in these mice.

DISCUSSION

Our findings indicate that cytotoxic lymphocytes (CTLs) persist in the brain over the long term after injury and contribute to the progressive deterioration of neurological/motor function, but not cognitive function, along with spinal cord damage. B cells likely play a regulatory role in TBI, while circulating autoantibodies against myelin/dsDNA do not seem to contribute to neurological outcomes.

TBI has recently been linked to the development of neurodegenerative conditions later in life (Bazarian et al., 2009; Lunny et al., 2014) for which chronic inflammation is considered a contributing factor (Amor et al., 2010). However, the role of lymphocytes that are known to cause pathology in some of these conditions has not been examined in chronic TBI. Evidence for the deleterious effects of CTLs in TBI comes from our findings in which mice that are genetically deficient or pharmacologically depleted of CD8$^+$ T cells had improved neurological outcomes and reduced myelin pathology in the spinal cord over 8 weeks. While no evidence of improved cognition was found in CD8$^+$ T cell-depleted mice, it is possible that cognitive changes may have occurred earlier (Siebold et al., 2018). In experimental stroke, mice displayed improved behavioral function and decreased neuronal loss following the depletion of CD8$^+$ T cells, albeit within a much shorter time frame (7–14 days) (Mracsko et al., 2014). β2m$^{-/-}$ mice lack cell surface expression of MHC class I, which plays a role in reducing the synaptic plasticity of surviving neurons and circuits. KbDb$^{-/-}$ and PirB$^{-/-}$ mice that lack MHC class I expression have smaller infarcts and enhanced motor recovery after stroke (Adelson et al., 2012). The improved recovery due to the lack of efficient MHC class I expression in β2m$^{-/-}$ mice could be due to both dampened CD8$^+$ T cell function and improved synaptic plasticity within the parietal cortex. However, we have also shown that depletion of CD8$^+$ T cells improves outcomes after TBI, which confirms that CD8$^+$ T cells are the cause of long-term neurological impairment after TBI.

CD8$^+$ T cells likely mediate their harmful effects and promote neuronal/myelin degeneration via GrB/perforin pathways. A recent TBI study found that CD8$^+$ T cells infiltrated early at 24 h (promoted by astrocyte-derived IL-15) and secreted GrB, causing the activation of caspase-3/poly ADP ribose polymerase (PARP) pathways, which led to neuronal apoptosis (Wu et al., 2018). Increased GrB expression (which correlated with infiltrated CD8$^+$ T cells) has also been observed in a rat model of SCI (Chaitanya et al., 2009) and ischemic stroke (Chaitanya et al., 2010). Our findings are supported by a recent SCI study, which found that perforin (mainly produced by CD8$^+$ T cells) causes inflammation and blood-spinal cord barrier damage, as perforin$^{-/-}$ mice had improved outcomes, in the acute/subacute phase (Liu et al., 2019). This is important since it confirms that functionally active CD8$^+$ T cells that secrete perforin/GrB, as observed in our TBI study, can promote secondary damage in the CNS. Similar findings were reported at 1 week post-ischemic stroke in perforin$^{-/-}$ mice (Mracsko et al., 2014). The Mracsko et al. (2014) study also found that antigen-dependent activation

(D) Multiplex plasma cytokine analysis revealing a trending increase in (i) Th2-related anti-inflammatory cytokine IL-4 in the CD8 depleted mice (n = 8–9 biological replicates) relative to IgG2b control (n = 7–8 biological replicates). (ii) Monocyte chemoattractant protein-1 (MCP-1) was also increased, whereas (iii) KC was decreased in the CD8 depleted mice (n = 8–9 biological replicates) compared to IgG2b isotype control (n = 6–10 biological replicates).
(E) Autoantibodies against (i) MOG, (ii) PLP, and (iii) dsDNA were elevated in the CD8 depleted mice (n = 8–10 biological replicates/group) after TBI, measured by ELISA.
*$p < 0.05$, **$p < 0.01$, and ***$p < 0.001$. Unpaired two-tailed t test. Error bars represent SEMs.
See also Figures S2, S5, and S6.

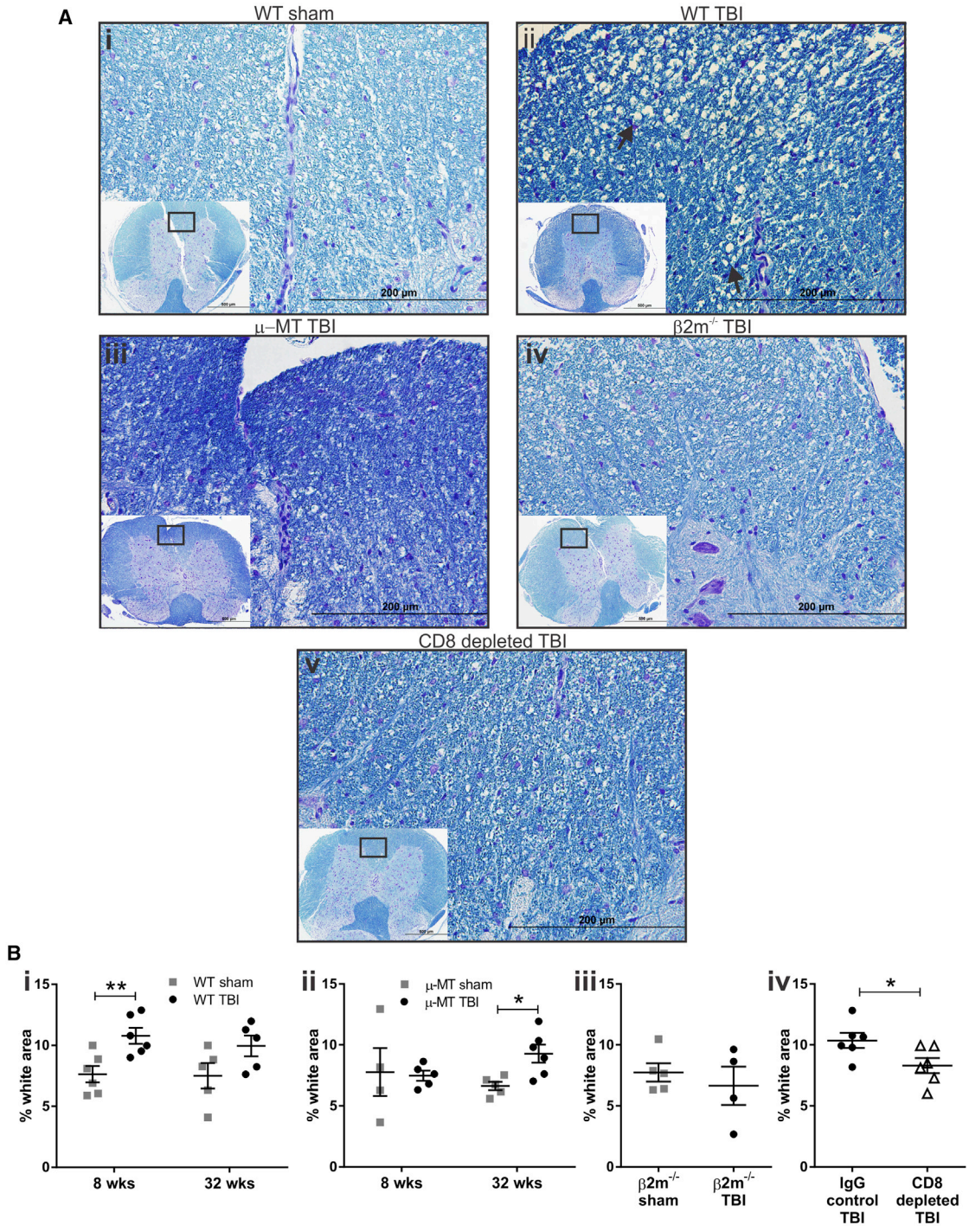

Figure 7. Mice Devoid of CD8$^+$ T Cells Show Reduced Myelin Vacuolization in the Spinal Cord 8 Weeks after TBI

(A) Representative LFB-stained spinal cord images (×400 magnification, scale bar, 200 μm, of the boxed region depicted in the smaller image; ×100 magnification, scale bar, 500 μm) showing myelin vacuolization (arrows) in (i) sham and (ii) injured WT mice and in (iii) μ-MT, (iv) β2m$^{-/-}$, and (v) CD8$^+$ T cell-depleted mice, at 8 weeks post-TBI.

(B) Quantitation of LFB staining revealed an increased percentage of myelin vacuoles (% white area) in (i) WT mice (n = 5–6 biological replicates) at 8 weeks but not 32 weeks, and (ii) μ-MT mice (n = 4–6 biological replicates) at 32 weeks but not 8 weeks post-TBI, compared to sham controls; they were decreased in (iv) CD8$^+$ T cell-depleted mice (n = 6 biological replicates) at 8 weeks relative to isotype control (n = 6 biological replicates). No differences in the percentage of white area were seen between (iii) β2m$^{-/-}$ TBI (n = 4 biological replicates) and sham-operated mice (n = 5 biological replicates).

*p < 0.05 and **p < 0.01. Unpaired two-tailed t test. Error bars represent SEMs.

was necessary for the neurotoxic effects elicited by $CD8^+$ T cells, and that the Th1 pro-inflammatory cytokine response had a minor role (compared to perforin) in mediating neuronal death by $CD8^+$ T cells, although Th17 cytokines were not investigated.

The trending (non-significant) increase in GrB^+ effector memory $CD4^+$ T cells suggests that a proportion of $CD4^+$ T cells are functionally active and producing GrB, but not to the extent of that of $CD8^+$ T cells. $CD4^+$ T cells that secrete GrB/perforin are termed $CD4^+$ CTLs (small subset of $CD4^+$ T cells) and adapt a similar cytotoxic function as $CD8^+$ CTLs (Takeuchi and Saito, 2017). Therefore, their function is that of a CTL and are likely activated along with $CD8^+$ CTLs, as has been identified in conditions in which cytotoxic $CD8^+$ T cells have a prime role (e.g., viral infection) (Takeuchi and Saito, 2017). There is still a great deal that is unknown about the function of these $CD4^+$ CTL and differentiation. The cytokine microenvironment (e.g., IL-17) and antigen stimulation, which we have proposed activate $CD8^+$ T cells, are also likely to promote the differentiation of $CD4^+$ T cells to their $CD4^+$ CTL phenotype (Takeuchi and Saito, 2017). Hence, it is interesting but perhaps not that surprising that GrB^+CD4^+ CTLs are slightly elevated along with a significant increase in GrB^+CD8^+ CTLs (and GrB^+ NK cells) in our model of TBI, and it further supports that cytotoxic-mediated damage almost certainly occurs in TBI during the chronic phase.

Th17-like cells/responses (e.g., IL-17A, IL-21) can enhance the cytotoxicity of $CD8^+$ T cells by enhancing GrB (and A) gene expression, as shown in other conditions (Acharya et al., 2016; Duan et al., 2012). That we observed an increase in IL-17 and IFN-γ-producing $CD4^+$ T cells in the brain at 1 week post-TBI, which preceded the increase in GrB^+CD8^+ T cells at 8 weeks, suggests that Th17 cells may be driving the cytotoxicity of $CD8^+$ T cells. $CD4^+$ IL-17-producing cells are known to promote cellular migration across the BBB and have a role in neuro-autoimmune diseases such as MS (Kebir et al., 2007). A recent study using the controlled cortical impact (CCI) model showed an increase in Th1/Th17 polarization in the injured brain and blood up to 3 weeks post-TBI, thereby strengthening our hypothesis that a Th17 response is a relevant component of the inflammatory response in TBI (Braun et al., 2017).

Therefore, we propose that direct cytolytic pathways (i.e., GrB/perforin) provide the means by which $CD8^+$ T cells mediate neuronal/myelin damage at the chronic phase of TBI, which may be enhanced by Th17-type responses at an earlier stage. The increased expression of GrB in $CD8^+$ T cells is an important finding, given that it implies that these $CD8^+$ T cells are activated (effector memory status) and functional (release GrB in response to stimuli) in the injured brain. This has provided insights into the mechanism by which $CD8^+$ T cells are likely potentiating their detrimental effects in TBI. It would be important for future studies to further investigate the GrB/perforin pathway and IL-17-related pathways in TBI. $GrB^{-/-}$ and $perforin^{-/-}$ mice would be required to assess whether the damage is definitively mediated by these cytotoxic agents, as our findings suggest. Further characterization of these $CD8^+$ T cells is also of interest to determine whether different subsets of $CD8^+$ T cells have distinct roles in TBI (e.g., by adoptive transfer of Tc1, Tc2, or Tc17 subsets), which would further complement our findings. It was of interest that the majority of $CD3^+$ T cells in the brain at the chronic phase post-TBI were $CD4^-CD8^-$ T cells (i.e., double negative or gamma delta T cells) (Gelderblom et al., 2009; Shichita et al., 2009). This has not previously been reported in TBI, and the functional role of these cells is not clear, but perhaps these cells have an immunoregulatory capacity (also referred to as double negative [DN] Tregs), as seen in many inflammatory conditions (Hillhouse et al., 2013).

The role of the classic Th2 cytokine IL-13 is surprisingly unexplored in the context of brain injury. The reduction of IL-13 in WT and μ-MT mice but its elevation in mice deficient in $CD8^+$ T cells suggests a beneficial role for this cytokine after TBI. Injured $CD8^+$ T cell-depleted mice showed increased MCP-1, which is associated with Th2 polarization and enhanced IL-4 production by T cells (Deshmane et al., 2009) and correlates with the increased trend in Th2-related IL-4 cytokine levels in these mice. Furthermore, we saw that effector memory $CD4^+$ T cells together with the Th2-related cytokines were increased in $CD8^+$ T cell-deficient/-depleted mice post-TBI. These increased $CD4^+$ T cells were not Treg cells, therefore suggesting that the lack of "pathogenic" CD8 T cells was likely responsible for the beneficial effects observed. However, it is plausible that these increased $CD4^+$ T cells could be skewed toward an anti-inflammatory Th2 phenotype promoting neuroprotection, as indicated by a CNS injury study (Walsh et al., 2015). $CD4^+$ T cell depletion was not sufficient to mitigate an overall improvement in function after TBI, and yet depletion/genetic deletion of $CD8^+$ T cells are both neuroprotective. Therefore, this shows that while initially $CD4^+IL17^+$ cells and later $CD4^+GrB^+$ cells are increased at the site of injury, possibly contributing to the self-renewal and enhanced cytotoxicity of $CD8^+$ T cells, it is ultimately the $CD8^+$ T cells that are detrimental after TBI.

Injured μ-MT mice displayed severe neurological/motor dysfunction, a robust immune response along with prominent myelin vacuolization in the spinal cord up to 32 weeks, which contrasts reports described in chronic SCI models (Ankeny et al., 2009; Doyle et al., 2015). Consistent with our findings however, μ-MT mice subjected to ischemic stroke demonstrated increased infarct sizes, an impaired functional outcome, and a similar T cell-directed response along with increased inflammatory cells (Ren et al., 2011). In μ-MT mice, it is probable that the increased $CD4^+$ NKT-like cells represent type 1 "invariant" NKT cells as they are known to produce both Th1 and Th2 cytokines and promote $CD8^+$ T cell responses (Kumar and Delovitch, 2014), which were also increased in these mice and may explain why the inflammatory response and cytokine profile in the μ-MT mice differed from WT mice.

Previous studies have shown that CNS injury induces an autoreactive response, including autoantibodies directed against several neuronal and/or myelin antigens (Ankeny et al., 2006; Ngankam et al., 2011; Ortega et al., 2015; Rudehill et al., 2006; Shibata et al., 2012). We initially linked increased circulating autoantibodies against myelin and dsDNA antigens to the progressive neurological defects observed in these WT mice from 8 to 32 weeks post-TBI. However, because the absence of a humoral response in μ-MT mice led to a worse outcome after TBI and the depletion of $CD8^+$ T cells in mice prompted an increase in antibodies but improved outcomes, we speculate that B cells and autoreactive antibodies may actually be protective. B cells can secrete IL-10 and promote neuroprotection, as was shown

following acute middle cerebral artery occlusion (MCAO) (Bodhankar et al., 2013, 2015). Autoantibodies can elicit neuroprotective effects by facilitating the removal of damaged cells at the lesion site and augmenting remyelination (Vargas et al., 2010). Although this study did not observe beyond 8 months post-TBI, we cannot exclude the possibility that the elevated circulating autoantibodies together with an increase in $CD4^+IL17^+$ T cells (Th17) in the brain may trigger autoimmune disease at a later stage or possibly in response to another stimulus (i.e., subsequent head trauma). This warrants further investigation into whether there is a clear link between TBI and autoimmunity.

Short-term studies have reported that mice subjected to TBI exhibit slow mobility, gait impairment, and unilateral movements (lateropulsion), similar to those seen in the present chronic study (Fujimoto et al., 2004; Neumann et al., 2009). On the contrary, the intriguing display of tail weakness or tail muscle spasms as a result of TBI more closely resembles symptoms of an SCI model in which tail spasms progressively develop over 12 weeks (Kapitza et al., 2012) and CNS autoimmune disease (Tripathi et al., 2010). In particular, these long-term behavioral changes overlap in part with symptoms of Th17-dominated "atypical" experimental autoimmune encephalomyelitis (EAE) disease (Abromson-Leeman et al., 2004; Rothhammer et al., 2011). Prolonged sensorimotor deficits have been described up to 12–14 months post-CCI, but only through visually assessed tests (Shelton et al., 2008).

A recent study described long-term motor impairments over 12 weeks in a rat model of TBI and TBI-induced spinal cord damage at 12 weeks, but not at the earlier 1 week time point (Wright et al., 2017), akin to our results. Myelin vacuolization has not previously been reported in TBI, but it has been observed in the spinal cords of mice with SCI or EAE and can occur adjacent to demyelination in these conditions (Saadoun et al., 2008). It is likely that the vacuolization we observed is not only due to a loss of descending nerve fibers as a consequence of the initial injury but is also a result of the pathogenic $CD8^+$ T cell response detected in the brain (since $CD8^+$ T cell-depleted mice were protected), which contribute to the destruction of these descending nerve fibers originating in the cerebral cortex. It would be of interest to further investigate myelin vacuolization in other regions such as the cerebral cortex or sciatic nerve (peripheral nervous system). The loss of oligodendrocytes has been associated with myelin vacuolization (Pohl et al., 2011) in which the mechanism could be via destructive $CD8^+$ T cells (Mars et al., 2011). Furthermore, considering that $CD8^+$ T cell-deficient/-depleted mice did not display myelin vacuolization at 8 weeks after TBI, whereas μ-MT mice show this phenotype at 32 weeks, we suggest that B cells are playing a dual secondary role—perhaps acting as effective helpers to $CD8^+$ T cells following TBI but also by secreting neuroprotective cytokines at the later time point. This could explain the protection in μ-MT mice at 8 weeks but not at 32 weeks, as $CD8^+$ T cells may require priming by B cells for an efficient response against myelin in the spinal cord at the 8-week time point.

There are several existing therapies that may prevent these deleterious long-term consequences of TBI. Natalizumab, an approved drug for the treatment of MS, inhibits lymphocyte migration into the CNS by targeting α4 integrins. A promising stroke trial showed prolonged functional improvement over 90 days with natalizumab treatment compared to placebo (Elkins et al., 2017). Levodopa (a dopaminergic drug used for Parkinson disease) was also found to enhance motor function in stroke patients (Scheidtmann et al., 2001) and in a case of severe chronic TBI (Haig and Ruess, 1990) with paralysis. Its effects have been partially attributed to its ability to specifically reduce $CD8^+$ T cells and pro-inflammatory cytokines in the brain after stroke (Kuric and Ruscher, 2014). The therapeutic potential of anti-CD8 antibodies in CNS injury has not been explored thus far and is promising, given that such therapies are already available and are well tolerated in humans. Targeting pro-inflammatory T cells (e.g., by natalizumab or anti-IL-17 antibodies) or specifically abrogating the $CD8^+$ T cell response (e.g., by anti-CD8 antibodies shown here or levodopa) within a specified time window could prevent chronic neurodegeneration and improve outcomes after TBI.

In conclusion, we provide evidence of the causal relation between the adaptive immune response and late-onset neurodegeneration following brain injury. We postulate that after TBI, a Th17 response drives cytotoxic T cell activity in the brain stimulating granzyme B/perforin effector pathways, which contributes to continual neuronal damage, myelin pathology, and concomitant neurological dysfunction over an extended period. It is likely that these effector memory cells are acting in an antigen-dependent manner, given their persistent presence in the brain. Although the antigen(s) are not identified, it is reasonable to suggest that the Th17-driven $CD8^+$ T cell response may instigate neurodegeneration in other chronic inflammatory conditions affecting the brain. That the $CD8^+$ T depletion resulted in significant protection against the long-term consequences of TBI provides impetus to explore this as a treatment paradigm for TBI and possibly other neuroinflammatory conditions.

STAR★METHODS

Detailed methods are provided in the online version of this paper and include the following:

- KEY RESOURCES TABLE
- LEAD CONTACT AND MATERIALS AVAILABILITY
- EXPERIMENTAL MODEL AND SUBJECT DETAILS
  - Animals
- METHOD DETAILS
  - Controlled cortical impact model for inducing TBI
  - Functional assessment
  - Morris water maze (MWM) cognitive testing
  - Preparation of brain derived immune cells
  - Flow cytometric analysis
  - CD8 antibody depletion
  - CD4 antibody depletion
  - Blood collection
  - Detection of serum autoantibodies via ELISA
  - Multiplex cytokine assay
  - Histology and microscopy imaging
- QUANTIFICATION AND STATISTICAL ANALYSIS
  - Statistical analysis
  - Quantification of myelin vacuolisation in spinal cord sections
- DATA AND CODE AVAILABILITY

SUPPLEMENTAL INFORMATION

Supplemental Information can be found online at https://doi.org/10.1016/j.celrep.2019.09.046.

ACKNOWLEDGMENTS

The authors acknowledge the facilities, and scientific and technical assistance of Mr. Steve Cody at Monash Micro Imaging and members of the AMREP Flow Cytometry Core Facility at Monash University. We also acknowledge Dr. Rachael Borg, Dr. Evelyn Tsantikos, Dr. Jie-Yu Chung, Dr. Zeyad Nasa, Professor Magdalena Plebanski, Dr. Jennifer Boer, and Volga Tarlac for their assistance with experiments and for technical assistance. We acknowledge Professor Fabienne Mackay for supplying the μ-MT mice, Dr. Linda Wakim for the design of the antibody depletion experiment, Professor Joseph Trapani and Dr. Vivien Sutton (Peter MacCallum Cancer Centre) for help with the GrB and FasL analyses, and Dr. Nigel Jones and Dr. Bridgette Semple for assistance with the Morris water maze procedure. This study was supported by grants (APP1045755 and APP1126636) and a Fellowship (APP1044152) awarded to R.L.M. by the NHMRC of Australia, and by a Monash University, Faculty of Medicine, Nursing, and Health Sciences, Early Career Strategic Grant awarded to M.S.

AUTHOR CONTRIBUTIONS

M.D. contributed to the experimental design, executed experiments, analyzed the data, and wrote the manuscript. A.G., A.E.A., D.F.D., H.H., F.M., P.L., and J.G. assisted with the experiments. F.A. provided intellectual input. M.S. provided intellectual input, experimental design, and experiments, analyzed the data, and drafted and edited the manuscript. R.L.M. provided intellectual input, analyzed the data, and drafted and edited the manuscript.

DECLARATION OF INTERESTS

The authors declare no competing interests.

Received: December 19, 2017
Revised: August 8, 2019
Accepted: September 16, 2019
Published: October 29, 2019

REFERENCES

Abromson-Leeman, S., Bronson, R., Luo, Y., Berman, M., Leeman, R., Leeman, J., and Dorf, M. (2004). T-cell properties determine disease site, clinical presentation, and cellular pathology of experimental autoimmune encephalomyelitis. Am. J. Pathol. *165*, 1519–1533.

Acharya, D., Wang, P., Paul, A.M., Dai, J., Gate, D., Lowery, J.E., Stokic, D.S., Leis, A.A., Flavell, R.A., Town, T., et al. (2016). Interleukin-17A Promotes CD8+ T Cell Cytotoxicity To Facilitate West Nile Virus Clearance. J. Virol. *91*, e01529-16.

Adelson, J.D., Barreto, G.E., Xu, L., Kim, T., Brott, B.K., Ouyang, Y.-B., Naserke, T., Djurisic, M., Xiong, X., Shatz, C.J., and Giffard, R.G. (2012). Neuroprotection from stroke in the absence of MHCI or PirB. Neuron *73*, 1100–1107.

Amor, S., Puentes, F., Baker, D., and van der Valk, P. (2010). Inflammation in neurodegenerative diseases. Immunology *129*, 154–169.

Ankeny, D.P., Lucin, K.M., Sanders, V.M., McGaughy, V.M., and Popovich, P.G. (2006). Spinal cord injury triggers systemic autoimmunity: evidence for chronic B lymphocyte activation and lupus-like autoantibody synthesis. J. Neurochem. *99*, 1073–1087.

Ankeny, D.P., Guan, Z., and Popovich, P.G. (2009). B cells produce pathogenic antibodies and impair recovery after spinal cord injury in mice. J. Clin. Invest. *119*, 2990–2999.

Bazarian, J.J., Cernak, I., Noble-Haeusslein, L., Potolicchio, S., and Temkin, N. (2009). Long-term neurologic outcomes after traumatic brain injury. J. Head Trauma Rehabil. *24*, 439–451.

Beck, K.D., Nguyen, H.X., Galvan, M.D., Salazar, D.L., Woodruff, T.M., and Anderson, A.J. (2010). Quantitative analysis of cellular inflammation after traumatic spinal cord injury: evidence for a multiphasic inflammatory response in the acute to chronic environment. Brain *133*, 433–447.

Bodhankar, S., Chen, Y., Vandenbark, A.A., Murphy, S.J., and Offner, H. (2013). IL-10-producing B-cells limit CNS inflammation and infarct volume in experimental stroke. Metab. Brain Dis. *28*, 375–386.

Bodhankar, S., Chen, Y., Lapato, A., Vandenbark, A.A., Murphy, S.J., Saugstad, J.A., and Offner, H. (2015). Regulatory CD8(+)CD122 (+) T-cells predominate in CNS after treatment of experimental stroke in male mice with IL-10-secreting B-cells. Metab. Brain Dis. *30*, 911–924.

Bramlett, H.M., and Dietrich, W.D. (2015). Long-Term Consequences of Traumatic Brain Injury: Current Status of Potential Mechanisms of Injury and Neurological Outcomes. J. Neurotrauma *32*, 1834–1848.

Braun, M., Vaibhav, K., Saad, N., Fatima, S., Brann, D.W., Vender, J.R., Wang, L.P., Hoda, M.N., Baban, B., and Dhandapani, K.M. (2017). Activation of Myeloid TLR4 Mediates T Lymphocyte Polarization after Traumatic Brain Injury. J. Immunol. *198*, 3615–3626.

Bromley-Brits, K., Deng, Y., and Song, W. (2011). Morris water maze test for learning and memory deficits in Alzheimer's disease model mice. J. Vis. Exp. (*53*), 2920.

Callaway, J.K., Jones, N.C., and Royse, C.F. (2012). Isoflurane induces cognitive deficits in the Morris water maze task in rats. Eur. J. Anaesthesiol. *29*, 239–245.

Chaitanya, G.V., Kolli, M., and Babu, P.P. (2009). Granzyme-b mediated cell death in the spinal cord-injured rat model. Neuropathology *29*, 270–279.

Chaitanya, G.V., Schwaninger, M., Alexander, J.S., and Babu, P.P. (2010). Granzyme-b is involved in mediating post-ischemic neuronal death during focal cerebral ischemia in rat model. Neuroscience *165*, 1203–1216.

Christianson, G.J., Brooks, W., Vekasi, S., Manolfi, E.A., Niles, J., Roopenian, S.L., Roths, J.B., Rothlein, R., and Roopenian, D.C. (1997). Beta 2-microglobulin-deficient mice are protected from hypergammaglobulinemia and have defective antibody responses because of increased IgG catabolism. J. Immunol. *159*, 4781–4792.

Dardiotis, E., Hadjigeorgiou, G.M., Paterakis, K., Fountas, K., and Karanikas, V. (2012). Traumatic Brain Injury and Inflammation: Emerging Role of Innate and Adaptive Immunity (INTECH Open Access Publisher).

Deshmane, S.L., Kremlev, S., Amini, S., and Sawaya, B.E. (2009). Monocyte chemoattractant protein-1 (MCP-1): an overview. J. Interferon Cytokine Res. *29*, 313–326.

Doyle, K.P., Quach, L.N., Solé, M., Axtell, R.C., Nguyen, T.V., Soler-Llavina, G.J., Jurado, S., Han, J., Steinman, L., Longo, F.M., et al. (2015). B-lymphocyte-mediated delayed cognitive impairment following stroke. J. Neurosci. *35*, 2133–2145.

Duan, M.C., Huang, Y., Zhong, X.N., and Tang, H.J. (2012). Th17 cell enhances CD8 T-cell cytotoxicity via IL-21 production in emphysema mice. Mediators Inflamm. *2012*, 898053.

Elkins, J., Veltkamp, R., Montaner, J., Johnston, S.C., Singhal, A.B., Becker, K., Lansberg, M.G., Tang, W., Chang, I., Muralidharan, K., et al. (2017). Safety and efficacy of natalizumab in patients with acute ischaemic stroke (ACTION): a randomised, placebo-controlled, double-blind phase 2 trial. Lancet Neurol. *16*, 217–226.

Fujimoto, S.T., Longhi, L., Saatman, K.E., Conte, V., Stocchetti, N., and McIntosh, T.K. (2004). Motor and cognitive function evaluation following experimental traumatic brain injury. Neurosci. Biobehav. Rev. *28*, 365–378.

Gelderblom, M., Leypoldt, F., Steinbach, K., Behrens, D., Choe, C.U., Siler, D.A., Arumugam, T.V., Orthey, E., Gerloff, C., Tolosa, E., and Magnus, T. (2009). Temporal and spatial dynamics of cerebral immune cell accumulation in stroke. Stroke *40*, 1849–1857.

Godfrey, D.I., MacDonald, H.R., Kronenberg, M., Smyth, M.J., and Van Kaer, L. (2004). NKT cells: what's in a name? Nat. Rev. Immunol. *4*, 231–237.

Gonzalez-Quintela, A., Alende, R., Gude, F., Campos, J., Rey, J., Meijide, L.M., Fernandez-Merino, C., and Vidal, C. (2008). Serum levels of immunoglobulins

(IgG, IgA, IgM) in a general adult population and their relationship with alcohol consumption, smoking and common metabolic abnormalities. Clin. Exp. Immunol. *151*, 42–50.

Haig, A.J., and Ruess, J.M. (1990). Recovery from vegetative state of six months' duration associated with Sinemet (levodopa/carbidopa). Arch. Phys. Med. Rehabil. *71*, 1081–1083.

Hillhouse, E., Delisle, J.-S., and Lesage, S. (2013). Immunoregulatory CD4- CD8- T cells as a potential therapeutic tool for transplantation, autoimmunity, and cancer. Front. Immunol. *4*, 6.

Hurn, P.D., Subramanian, S., Parker, S.M., Afentoulis, M.E., Kaler, L.J., Vandenbark, A.A., and Offner, H. (2007). T- and B-cell-deficient mice with experimental stroke have reduced lesion size and inflammation. J. Cereb. Blood Flow Metab. *27*, 1798–1805.

Jassam, Y.N., Izzy, S., Whalen, M., McGavern, D.B., and El Khoury, J. (2017). Neuroimmunology of Traumatic Brain Injury: Time for a Paradigm Shift. Neuron *95*, 1246–1265.

Jazayeri, M.H., Pourfathollah, A.A., Rasaee, M.J., Porpak, Z., and Jafari, M.E. (2013). The concentration of total serum IgG and IgM in sera of healthy individuals varies at different age intervals. Biomed. Aging Pathol. *3*, 241–245.

Kapitza, S., Zörner, B., Weinmann, O., Bolliger, M., Filli, L., Dietz, V., and Schwab, M.E. (2012). Tail spasms in rat spinal cord injury: changes in interneuronal connectivity. Exp. Neurol. *236*, 179–189.

Kebir, H., Kreymborg, K., Ifergan, I., Dodelet-Devillers, A., Cayrol, R., Bernard, M., Giuliani, F., Arbour, N., Becher, B., and Prat, A. (2007). Human TH17 lymphocytes promote blood-brain barrier disruption and central nervous system inflammation. Nat. Med. *13*, 1173–1175.

Kitamura, D., Roes, J., Kühn, R., and Rajewsky, K. (1991). A B cell-deficient mouse by targeted disruption of the membrane exon of the immunoglobulin mu chain gene. Nature *350*, 423–426.

Kruisbeek, A.M. (2001). In Vivo Depletion of CD4- and CD8-Specific T Cells. Curr. Protoc. Immunol. *Chapter 4*, Unit 4.1.

Kumar, V., and Delovitch, T.L. (2014). Different subsets of natural killer T cells may vary in their roles in health and disease. Immunology *142*, 321–336.

Kuric, E., and Ruscher, K. (2014). Reduction of rat brain CD8+ T-cells by levodopa/benserazide treatment after experimental stroke. Eur. J. Neurosci. *40*, 2463–2470.

Liu, Z., Zhang, H., Xia, H., Wang, B., Zhang, R., Zeng, Q., Guo, L., Shen, K., Wang, B., Zhong, Y., et al. (2019). CD8 T cell-derived perforin aggravates secondary spinal cord injury through destroying the blood-spinal cord barrier. Biochem. Biophys. Res. Commun. *512*, 367–372.

Lunny, C.A., Fraser, S.N., and Knopp-Sihota, J.A. (2014). Physical trauma and risk of multiple sclerosis: a systematic review and meta-analysis of observational studies. J. Neurol. Sci. *336*, 13–23.

Maas, A.I., Stocchetti, N., and Bullock, R. (2008). Moderate and severe traumatic brain injury in adults. Lancet Neurol. *7*, 728–741.

Mars, L.T., Saikali, P., Liblau, R.S., and Arbour, N. (2011). Contribution of CD8 T lymphocytes to the immuno-pathogenesis of multiple sclerosis and its animal models. Biochim. Biophys. Acta *1812*, 151–161.

Mracsko, E., Liesz, A., Stojanovic, A., Lou, W.P., Osswald, M., Zhou, W., Karcher, S., Winkler, F., Martin-Villalba, A., Cerwenka, A., and Veltkamp, R. (2014). Antigen dependently activated cluster of differentiation 8-positive T cells cause perforin-mediated neurotoxicity in experimental stroke. J. Neurosci. *34*, 16784–16795.

Nasa, Z., Chung, J.Y., Chan, J., Toh, B.H., and Alderuccio, F. (2012). Nonmyeloablative conditioning generates autoantigen-encoding bone marrow that prevents and cures an experimental autoimmune disease. Am. J. Transplant. *12*, 2062–2071.

Neumann, M., Wang, Y., Kim, S., Hong, S.M., Jeng, L., Bilgen, M., and Liu, J. (2009). Assessing gait impairment following experimental traumatic brain injury in mice. J. Neurosci. Methods *176*, 34–44.

Ngankam, L., Kazantseva, N.V., and Gerasimova, M.M. (2011). [Immunological markers of severity and outcome of traumatic brain injury]. Zh. Nevrol. Psikhiatr. Im. S. S. Korsakova *111*, 61–65.

Ortega, S.B., Noorbhai, I., Poinsatte, K., Kong, X., Anderson, A., Monson, N.L., and Stowe, A.M. (2015). Stroke induces a rapid adaptive autoimmune response to novel neuronal antigens. Discov. Med. *19*, 381–392.

Plesnila, N. (2016). The immune system in traumatic brain injury. Curr. Opin. Pharmacol. *26*, 110–117.

Pohl, H.B., Porcheri, C., Mueggler, T., Bachmann, L.C., Martino, G., Riethmacher, D., Franklin, R.J., Rudin, M., and Suter, U. (2011). Genetically induced adult oligodendrocyte cell death is associated with poor myelin clearance, reduced remyelination, and axonal damage. J. Neurosci. *31*, 1069–1080.

Raad, M., Nohra, E., Chams, N., Itani, M., Talih, F., Mondello, S., and Kobeissy, F. (2014). Autoantibodies in traumatic brain injury and central nervous system trauma. Neuroscience *281*, 16–23.

Ren, X., Akiyoshi, K., Dziennis, S., Vandenbark, A.A., Herson, P.S., Hurn, P.D., and Offner, H. (2011). Regulatory B cells limit CNS inflammation and neurologic deficits in murine experimental stroke. J. Neurosci. *31*, 8556–8563.

Rothhammer, V., Heink, S., Petermann, F., Srivastava, R., Claussen, M.C., Hemmer, B., and Korn, T. (2011). Th17 lymphocytes traffic to the central nervous system independently of α4 integrin expression during EAE. J. Exp. Med. *208*, 2465–2476.

Rudehill, S., Muhallab, S., Wennersten, A., von Gertten, C., Al Nimer, F., Sandberg-Nordqvist, A.C., Holmin, S., and Mathiesen, T. (2006). Autoreactive antibodies against neurons and basal lamina found in serum following experimental brain contusion in rats. Acta Neurochir. (Wien) *148*, 199–205, discussion 205.

Saadoun, S., Bell, B.A., Verkman, A.S., and Papadopoulos, M.C. (2008). Greatly improved neurological outcome after spinal cord compression injury in AQP4-deficient mice. Brain *131*, 1087–1098.

Sashindranath, M., Samson, A.L., Downes, C.E., Crack, P.J., Lawrence, A.J., Li, Q.X., Ng, A.Q., Jones, N.C., Farrugia, J.J., Abdella, E., et al. (2011). Compartment- and context-specific changes in tissue-type plasminogen activator (tPA) activity following brain injury and pharmacological stimulation. Lab. Invest. *91*, 1079–1091.

Sashindranath, M., Sales, E., Daglas, M., Freeman, R., Samson, A.L., Cops, E.J., Beckham, S., Galle, A., McLean, C., Morganti-Kossmann, C., et al. (2012). The tissue-type plasminogen activator-plasminogen activator inhibitor 1 complex promotes neurovascular injury in brain trauma: evidence from mice and humans. Brain *135*, 3251–3264.

Sashindranath, M., Daglas, M., and Medcalf, R.L. (2015). Evaluation of gait impairment in mice subjected to craniotomy and traumatic brain injury. Behav. Brain Res. *286*, 33–38.

Scheidtmann, K., Fries, W., Müller, F., and Koenig, E. (2001). Effect of levodopa in combination with physiotherapy on functional motor recovery after stroke: a prospective, randomised, double-blind study. Lancet *358*, 787–790.

Semple, B.D., Noble-Haeusslein, L.J., Gooyit, M., Tercovich, K.G., Peng, Z., Nguyen, T.T., Schroeder, V.A., Suckow, M.A., Chang, M., Raber, J., and Trivedi, A. (2015). Early Gelatinase Activity Is Not a Determinant of Long-Term Recovery after Traumatic Brain Injury in the Immature Mouse. PLoS One *10*, e0143386.

Shelton, S.B., Pettigrew, D.B., Hermann, A.D., Zhou, W., Sullivan, P.M., Crutcher, K.A., and Strauss, K.I. (2008). A simple, efficient tool for assessment of mice after unilateral cortex injury. J. Neurosci. Methods *168*, 431–442.

Shibata, D., Cain, K., Tanzi, P., Zierath, D., and Becker, K. (2012). Myelin basic protein autoantibodies, white matter disease and stroke outcome. J. Neuroimmunol. *252*, 106–112.

Shichita, T., Sugiyama, Y., Ooboshi, H., Sugimori, H., Nakagawa, R., Takada, I., Iwaki, T., Okada, Y., Iida, M., Cua, D.J., et al. (2009). Pivotal role of cerebral interleukin-17-producing gammadeltaT cells in the delayed phase of ischemic brain injury. Nat. Med. *15*, 946–950.

Siebold, L., Obenaus, A., and Goyal, R. (2018). Criteria to define mild, moderate, and severe traumatic brain injury in the mouse controlled cortical impact model. Exp. Neurol. *310*, 48–57.

Sundman, M.H., Hall, E.E., and Chen, N.K. (2014). Examining the relationship between head trauma and neurodegenerative disease: A review

of epidemiology, pathology and neuroimaging techniques. J. Alzheimers Dis. Parkinsonism *4*, 137.

Takeuchi, A., and Saito, T. (2017). CD4 CTL, a Cytotoxic Subset of CD4$^+$ T Cells, Their Differentiation and Function. Front. Immunol. *8*, 194.

Tripathi, R.B., Rivers, L.E., Young, K.M., Jamen, F., and Richardson, W.D. (2010). NG2 glia generate new oligodendrocytes but few astrocytes in a murine experimental autoimmune encephalomyelitis model of demyelinating disease. J. Neurosci. *30*, 16383–16390.

Vargas, M.E., Watanabe, J., Singh, S.J., Robinson, W.H., and Barres, B.A. (2010). Endogenous antibodies promote rapid myelin clearance and effective axon regeneration after nerve injury. Proc. Natl. Acad. Sci. USA *107*, 11993–11998.

Walker, W.C., and Pickett, T.C. (2007). Motor impairment after severe traumatic brain injury: a longitudinal multicenter study. J. Rehabil. Res. Dev. *44*, 975–982.

Walsh, J.T., Hendrix, S., Boato, F., Smirnov, I., Zheng, J., Lukens, J.R., Gadani, S., Hechler, D., Gölz, G., Rosenberger, K., et al. (2015). MHCII-independent CD4+ T cells protect injured CNS neurons via IL-4. J. Clin. Invest. *125*, 699–714.

Weckbach, S., Neher, M., Losacco, J.T., Bolden, A.L., Kulik, L., Flierl, M.A., Bell, S.E., Holers, V.M., and Stahel, P.F. (2012). Challenging the role of adaptive immunity in neurotrauma: Rag1(-/-) mice lacking mature B and T cells do not show neuroprotection after closed head injury. J. Neurotrauma *29*, 1233–1242.

Weitzner, D.S., Engler-Chiurazzi, E.B., Kotilinek, L.A., Ashe, K.H., and Reed, M.N. (2015). Morris Water Maze Test: Optimization for Mouse Strain and Testing Environment. J. Vis. Exp. *100*, e52706.

Wright, D.K., Liu, S., van der Poel, C., McDonald, S.J., Brady, R.D., Taylor, L., Yang, L., Gardner, A.J., Ordidge, R., O'Brien, T.J., et al. (2017). Traumatic Brain Injury Results in Cellular, Structural and Functional Changes Resembling Motor Neuron Disease. Cereb. Cortex *27*, 4503–4515.

Wu, B., Matic, D., Djogo, N., Szpotowicz, E., Schachner, M., and Jakovcevski, I. (2012). Improved regeneration after spinal cord injury in mice lacking functional T- and B-lymphocytes. Exp. Neurol. *237*, 274–285.

Wu, L., Ji, N.N., Wang, H., Hua, J.Y., Sun, G.L., Chen, P.P., Hua, R., and Zhang, Y.M. (2018). Domino effect of IL-15 and CD8 T cell-mediated neuronal apoptosis in experimental traumatic brain injury. J. Neurotrauma. https://doi.org/10.1089/neu.2017.5607.

Yilmaz, G., Arumugam, T.V., Stokes, K.Y., and Granger, D.N. (2006). Role of T lymphocytes and interferon-gamma in ischemic stroke. Circulation *113*, 2105–2112.

Zijlstra, M., Bix, M., Simister, N.E., Loring, J.M., Raulet, D.H., and Jaenisch, R. (1990). Beta 2-microglobulin deficient mice lack CD4-8+ cytolytic T cells. Nature *344*, 742–746.

STAR★METHODS

KEY RESOURCES TABLE

REAGENT or RESOURCE	SOURCE	IDENTIFIER
Antibodies		
Rat monoclonal anti-mouse CD8 antibody (4SM16)	Thermo Fisher Scientific	Cat# 14-0195-82; RRID: AB_2637159
Biotinylated rabbit anti-rat IgG	Vector Laboratories	Cat# BA-4000; RRID: AB_2336206
Rat monoclonal anti-mouse CD8 (2.43)	WEHI antibody facility, Melbourne	N/A
Rat monoclonal anti-mouse CD4 (GK1.5)	WEHI antibody facility, Melbourne	N/A
Rat anti-mouse IgG2b isotype antibody	WEHI antibody facility, Melbourne	N/A
HRP conjugated goat anti-mouse IgG-Fc	Bethyl Laboratories	Cat# A90-131P; RRID: AB_67175
V450 hamster anti-mouse CD11c	BD biosciences	Cat# 560521; RRID: AB_1727423
PE/Cy7 rat anti-mouse CD11b	eBioscience	Cat# 25-0112-82; RRID: AB_469588
APC rat anti-mouse Gr1	BD biosciences	Cat# 553129; RRID: AB_398532
AF488 rat anti-mouse Gr1	eBioscience	Cat# 53-5931-82; RRID: AB_469918
APC-eFluor 780 rat anti-mouse MHCII (I-A/I-E)	eBioscience	Cat# 47-5321-82; RRID: AB_1548783
PerCP rat anti-mouse F4/80 /EMR1	R&D systems	Cat# FAB5580C; RRID: AB_2044654
PE rat anti-mouse CD45	BD biosciences	Cat# 553081; RRID: AB_394611
FITC rat anti-mouse CD8α	eBioscience	Cat# 11-0081-82; RRID: AB_464915
PE/Cy7 rat anti-mouse CD8α	eBioscience	Cat# 25-0081-82; RRID: AB_469584
APC rat anti-mouse CD8b.2	BioLegend	Cat# 140409; RRID: AB_10640731
FITC rat anti-mouse CD8b.2	BioLegend	Cat# 140403; RRID: AB_10641694
AF700 rat anti-mouse CD45R/B220	BD biosciences	Cat# 557957; RRID: AB_396957
APC rat anti-mouse CD45R/B220	BD biosciences	Cat# 553092; RRID: AB_398531
FITC rat anti-mouse CD19	eBioscience	Cat# 11-0193-82; RRID: AB_657666
APC-eFluor 780 rat anti-mouse CD3	eBioscience	Cat# 47-0032-82; RRID: AB_1272181
BV605 rat anti-mouse CD4	BD biosciences	Cat# 563151; RRID: AB_2687549
PerCP rat anti-mouse CD4	BD biosciences	Cat# 561090; RRID: AB_10562560
FITC rat anti-mouse CD4	eBioscience	Cat# 11-0042-81C; RRID: AB_464895
AF700 rat anti-mouse CD4 (RM4-4)	BioLegend	Cat# 116021; RRID: AB_2715957
AF700 hamster anti-mouse CD69	BD biosciences	Cat# 561238; RRID: AB_10611869
eFluor 450 hamster anti-mouse CD69	eBioscience	Cat# 48-0691-82; RRID: AB_10719430
V450 rat anti-mouse CD44	BD biosciences	Cat# 560452; RRID: AB_1645274
PE/Cy5 rat anti-mouse CD44	eBioscience	Cat# 15-0441-82; RRID: AB_468749
PerCP-Cy5.5 rat anti-mouse CD62L (L-selectin)	eBioscience	Cat# 45-0621-80; RRID: AB_996669
PE-CF594 rat anti-mouse CD62L	BD biosciences	Cat# 562404; RRID: AB_11154046
PE mouse anti-mouse NK1.1	eBioscience	Cat# 12-5941-82; RRID: AB_466050
AF700 mouse anti-mouse NK1.1	eBioscience	Cat# 56-5941-80; RRID: AB_2574504
PE hamster anti-mouse FasL (CD178)	BioLegend	Cat# 106605; RRID: AB_313278
AF647 mouse anti-human Granzyme B	BD biosciences	Cat# 561999; RRID: AB_10897997
PE mouse anti-human Granzyme B	Sanquin	Cat# M2289; RRID: AB_2114694
APC rat anti-mouse FoxP3	eBioscience	Cat# 17-5773-80; RRID: AB_469456
PE/Cy7 rat anti-mouse CD25	BD biosciences	Cat# 552880; RRID: AB_394509
PerCP-eFluor 710 mouse anti-mouse LAP	eBioscience	Cat# 46-9821-82; RRID: AB_10853808
AF488 rat anti-mouse IL-17A	eBioscience	Cat# 53-7177-81; RRID: AB_763579
eFluor 450 rat anti-mouse IFNγ	eBioscience	Cat# 48-7311-80; RRID: AB_1834367

(*Continued on next page*)

Continued

REAGENT or RESOURCE	SOURCE	IDENTIFIER
Chemicals, Peptides, and Recombinant Proteins		
MOG_{35-55} peptide	GL Biochem (Shanghai) Ltd	Cat# 51716
$PLP_{139-151}$ peptide	GL Biochem (Shanghai) Ltd	Cat# 86603
PMA (Phorbol 12-myristate 13-acetate)	Sigma Aldrich	Cat# P1585
Ionomycin	Sigma Aldrich	Cat# I3909
Brefeldin A	Sigma Aldrich	Cat# B5936
Critical Commercial Assays		
Bio-Plex Pro Mouse Cytokine 23-Plex kit	Bio-Rad Laboratories	Cat# M60009RDPD
ImmPACT DAB Peroxidase (HRP) Substrate kit	Vector Laboratories	Cat# SK-4105
VECTASTAIN Elite ABC-HRP kit	Vector Laboratories	Cat# PK-6100
Live/Dead Fixable Aqua Dead Cell Stain kit	Life Technologies	Cat# L34957
Fixation/Permeabilisation buffer kit	eBioscience	Cat# 88-8824-00
Experimental Models: Organisms/Strains		
Mouse: C57BL/6J	Animal Resources Centre, WA	N/A
Mouse: μ-MT	Prof. Fabienne Mackay, Monash Animal Research Platform	N/A
Mouse: β2 m−/−	Australian Phenomics Facility	N/A
Software and Algorithms		
ImageJ	NIH	https://imagej.nih.gov/ij/
DigiGait analysis software v.12.2	Mouse Specifics Inc., USA	https://mousespecifics.com/digigait/
TopScan software	CleverSys, Inc	http://cleversysinc.com/CleverSysInc/csi_products/topscan-lite/
FlowJo VX version	Tree Star Inc. USA	https://www.flowjo.com/solutions/flowjo/
Bio-Plex Manager Software	Bio-Rad Laboratories Pty., Ltd. Australia	https://www.bio-rad.com/en-au/applications-technologies/bio-plex-data-analysis-software?ID=M15GLB15
GraphPad Prism (version 6.01)	GraphPad Software Inc. USA	https://www.graphpad.com/scientific-software/prism/

LEAD CONTACT AND MATERIALS AVAILABILITY

Further information and requests for resources and reagents should be directed to and will be fulfilled by the Lead Contact, Robert L. Medcalf (robert.medcalf@monash.edu).

This study did not generate new unique reagents.

EXPERIMENTAL MODEL AND SUBJECT DETAILS

Animals

All experiments involved adult male mice on a C57BL/6 background, and were approved by the Alfred Medical Research and Education Precinct (AMREP), Animal Ethics Committee in accordance with the Australian code of practice for the care and use of animals for scientific purposes. C57BL/6J WT mice were used aged between 7-13 weeks and were sourced from the Animal Resources Centre (ARC) in Western Australia. Beta-2 microglobulin-deficient ($\beta2m^{-/-}$) mice at 7-14 weeks of age were sourced from the Australian Phenomics Facility in Canberra, Australia. These mice lack major histocompatibility class I (MHC-I) molecules and therefore mature CD8+ T cells (Zijlstra et al., 1990). A limited cohort of these β2 $m^{-/-}$ mice were available as breeding was inefficient. μ-MT mice (9-17 weeks of age) were obtained from Prof. Fabienne Mackay and bred at the Monash Animal Research Platform (MARP) in Melbourne, Australia. These mice do not develop functional B cells (and therefore antibodies) due to the absence of the immunoglobulin μ-chain gene (Kitamura et al., 1991). Male mice were used for all experiments for all mouse strains (C57BL/6J, μ-MT and β2 $m^{-/-}$ mice). All animals were housed in specific pathogen-free facilities (≤six mice per cage) before surgery with food and water *ad libitum*, in a temperature-controlled environment with a 12 h light/12 h dark cycle. WT mice were randomly chosen and subjected to one treatment group each. β2 m−/− and μ-MT mice were obtained as per breeding availability and always randomly assigned to trauma and sham groups. Following surgery, mice were housed individually in cages with fitted split feeders and cage dividers. Animals were euthanized at specified time-points.

METHOD DETAILS

Controlled cortical impact model for inducing TBI

TBI was performed on mice using the CCI model (Sashindranath et al., 2011). Mice were anaesthetised intraperitoneally with 2,2,2-tribromoethanol solution (0.5 mg/kg; Sigma–Aldrich) and placed in a stereotaxic frame (Kopf, Tujunga, CA). A 1 cm sagittal incision was made to expose the skull using a scalpel and the skull was cleaned with hydrogen peroxide (6%). A craniotomy was then performed by drilling a 5mm diameter burr hole to expose the brain at coordinates, −2 mm anteroposterior and +2 mm mediolateral of bregma. Following craniotomy, a single blunt force trauma was induced on the exposed left parietal cortex at a 20° angle using a computer-driven cylindrical rod, at a velocity of 5 m/s with 150 ms dwell time and 2 mm impact depth. Bone wax was used to seal the exposed brain and the scalp incision was then sutured and treated with betadine. Sham mice were anaesthetised and underwent only the craniotomy procedure followed by suturing. A non-craniotomised sham group (sham NC) was included for one cohort (WT 8 week time-point) whereby mice did not undergo craniotomy or impact but were subjected to the anesthetic, scalp incision and suturing. Following surgery, mice were euthanized with urethane (3.3g/kg) at fixed time-points up to 32 weeks. For histology, mice were transcardially perfused with 20ml of PBS (pH 7.3) followed by 10% phosphate buffered formalin. Removed brain tissue was kept in 10% phosphate buffered formalin overnight at 4°C, then processed in a Shandon tissue processor overnight (alcohol cycle) and paraffin embedded.

Functional assessment

TBI and sham-operated mice were monitored and analyzed for neurological deficits weekly up to 32 weeks post-TBI. The neurological test that we devised was adapted partially from the modified neurological severity score (Fujimoto et al., 2004) as well as the classical scoring system for EAE (Nasa et al., 2012; Tripathi et al., 2010) to accommodate for unanticipated long-term deficits of TBI. Specifically, we assessed changes in mobility, unilateral movement, uneven gait, tail weakness, and tail spasms (see Video S1). An average cumulative score (i.e., each observation given a score of 1) was then determined over the period of time analyzed (t = 32 weeks: 4 week intervals). A maximum total cumulative score of 5 was achievable for each individual assessment (5 = most severe). Gait was assessed using the DigiGait^{TM} apparatus (Mouse Specifics Inc., USA) as described (Sashindranath et al., 2012, 2015). Briefly, mice were allowed to run freely on a transparent motorised treadmill for approximately 5 s at a constant speed of 15 cm/s. Visual recordings of paw placement from the ventral plane direction were quantitatively analyzed by DigiGait analysis software v.12.2 (Mouse Specifics Inc., USA). Various gait parameters are measured (including stride, stance, swing, brake, and propulsion) for each limb. Behavioral experiments were always conducted in the afternoon (2pm-5pm; light cycle), and the assessor was unaware of the treatment status of the mice during testing. Mice were acclimatised to the environment in the testing room for 15 min before testing commenced on any given session.

Morris water maze (MWM) cognitive testing

CD8 depleted, CD4 depleted and IgG2b control mice were assessed for changes in cognition (i.e., spatial learning/memory) by performing MWM testing at 7-8 weeks post-TBI. The MWM protocol was adapted from Bromley-Brits et al. (2011); Callaway et al. (2012); Semple et al. (2015), and Weitzner et al. (2015). Briefly, a 1.2 m diameter pool was filled with water (22°C) mixed with non-toxic white paint up to 30cm, and spatial cues were set around the edges of the pool (i.e., on day 1 onward). Mice were allowed to swim 2x 60 s with a visible platform (using a flag only on first trial) on the pre-training day (the day prior to day 1). This was followed by 4 days of training with 3 trials each, where mice were given 90 s to find a hidden platform (submerged 1.5cm). In the case that the mouse did not find the platform within 90 s, the mouse was gently guided to the platform and allowed to stay on the platform for 10 s (max 3 times). The position of the platform remained constant although the quadrant location was changed for each trial. A probe trial was then performed on the day 5, whereby mice were allowed to swim for 90 s with the platform removed from the pool, to determine if more time is spent in that relevant quadrant. An overhead mounted camera and TopScan software (CleverSys, Inc) was used to tack the animal in real time and measure the time taken to find platform, distance traveled, and swim velocity. Mice were acclimatised to the environment for at least 15 min, testing was conducted in the afternoon at the same time each day and the assessor was unaware of the treatment status of the mice during testing.

Preparation of brain derived immune cells

We devised a technique to isolate immune cells from brain tissue for flow cytometry by adapting a method previously described for spinal cord tissue (Beck et al., 2010). Brain tissue was separated into ipsilateral and contralateral hemispheres following gentle removal of the meninges using a cotton bud. Hemispheres were mechanically dissociated using fine scissors in HBSS+ (containing 1% BSA, 1M $CaCl_2$, 1M HEPES and 150mM $MgSO_4$) and centrifuged at 805 rcf for 3 minutes at 4°C. The pelleted tissue was enzymatically digested with collagenase/dispase (2mg/ml; Roche Life Science, Australia), TLCK (Tosyl-L-lysyl-chloromethane hydrochloride; 10μM) and DNase1 (1mg) (Sigma-Aldrich, Australia) in HBSS+ for 30 min in a 37°C water bath followed by addition of fetal bovine serum (FBS) to a final concentration of 10% (v/v) to stop enzyme activity. The tissue digest was filtered through a 70μm cell strainer, centrifuged at 805 rcf for 3 min and resuspended in 6 mL cold HBSS+ buffer. Density centrifugation was used to enrich cell populations. OptiPrep solution (Sigma-Aldrich, Australia) was initially diluted 1:1 with 10mM MOPS buffer (3-(N-morpholino) propanesulfonic acid) containing 0.15M NaCl. The cell suspension was then overlayed on an OptiPrep density gradient consisting of 4 different

dilutions (525, 375, 300 or 225 μl of optiprep solution to a total of 1.5 mL per dilution) that were prepared by layering the least dilute preparation to the most dilute preparation, and then centrifuged at 726 rcf for 20 min without braking, at 20°C. Myelin and debris were aspirated from the top layer allowing isolation of immune cells, which were washed with 7ml HBSS+, centrifuged at 726 rcf for 3 min (20°C) and resuspended in PBS with 2% FBS for immunostaining.

Flow cytometric analysis

Immune cells isolated from brain tissue (ipsilateral and contralateral hemispheres) or the cLN of mice subjected to TBI/sham procedure were analyzed by flow cytometry. Isolated immune cells from the brain (method described above) or single cell suspensions of the cLN (filtered through 70μm cell strainer and resuspended in PBS with 2% FBS) were stained (50μl/sample) with immune markers of inflammatory cells (microglia/macrophages, neutrophils, and dendritic cells (DC)) and lymphocytes (T and B cells, NKT-like cells) for 20 min at 4°C. The lymphocyte cocktail included the following antibodies (from eBioscience Inc. USA, unless otherwise specified); rat anti-mouse CD3 APC-eFluor 780, CD8a PEcy7 or CD8b.2 APC (BioLegend, USA), CD19 FITC, CD44 v450, CD62L PerCP-cy5.5, CD4 FITC or CD4 PerCP (BD, Australia) or CD4 BV605 (BD, Australia), CD45R/B220 APC (BD, Australia) or B220 biotinylated, mouse anti-mouse NK1.1 PE and/or hamster anti-mouse CD69 eFluor 450 or CD69 AF700 (BD, Australia). Inflammatory cell cocktail included the following antibodies, from eBioscience Inc. USA, unless otherwise specified; rat anti-mouse CD11b PEcy7, Gr1 APC (BD, Australia), or Gr1 AF488, CD8a FITC, or CD8b.2 APC (BioLegend, USA), CD45R/B220 AF700 (BD Biosciences), MHCII (I-A/I-E) APC-eFluor 780, CD45 PE (BD, Australia), F4/80/EMR1 PerCP (R&D Systems Inc., USA) and/or hamster anti-mouse CD11c v450 (BD, Australia). Cells were washed with PBS with 2% FBS (805 rcf for 3 min at 4°C), resuspended in LIVE/DEAD® Fixable Aqua dead cell stain (DCS: Life Technologies Australia Pty Ltd) solution and incubated for 15 min at 4°C. With the biotinylated anti-B220 antibody, a secondary streptavidin-PE/Cy7 antibody was added with the dead cell stain cocktail and incubated for 20 min (4°C). All samples were then washed with PBS with 2% FBS and fixed with 1% formaldehyde solution. Data were collected on a BD LSRFortessa cell analyzer at a total of 50,000 live events. Cell counts were determined using counts attained by the flow cytometer and adjusted to the quantity of sample acquired, and validated using CountBright absolute counting beads (Life Technologies). Because CD1d expression (ideally used for extensive NKT cell analysis) was not profiled, CD3+NK1.1+CD4+ cells are best described as CD4+ NKT-like cells as it is unclear whether these cells are CD1d-dependent or independent NKT cells (Godfrey et al., 2004).

For cytokine assessment using flow cytometry, isolated brain cells were stimulated with PMA/ionomycin and brefeldin A (Sigma Aldrich, Australia) for 5 h at 37°C. Following the incubation, cells were resuspended in PBS with 2% FBS and stained for surface markers including CD3 APC-eFluor 780, CD4 BV605, CD8 PEcy7 and DCS (same as lymphocyte cocktail above) for 20 min at 4°C. Brain cells were washed with PBS/2% FBS and then fixed and permeabilised with Fixation/Permeabilisation buffer kit (eBioscience) for 30 min at room temperature. Cells were washed with Permeabilisation wash buffer and incubated with rat anti-mouse IL-17A AF488 and rat anti-mouse IFN-γ eFluor450 (both from eBioscience Inc. USA) for 30 min at room temperature. Cells were washed with PBS/2% FBS and analyzed using the BD LSRFortessa as described above.

Treg cells and granzyme B expression were analyzed in isolated brain and cLN cells of antibody depleted cohorts and WT injured mice at the 8 week time-point, by intracellular flow cytometry techniques (following above protocol including intracellular staining steps shown in cytokine assessment section but without stimulation). Samples were stained with intracellular markers, FoxP3 APC (eBioscience, USA) and GrB PE (Sanquin) or GrB AF647 (BD Bioscience), in addition to lymphocyte surface markers (from eBioscience, USA, unless specified) including; CD3 APC-eFluor780, CD8b.2 FITC (Biolegend) or CD8a PEcy7, CD4 (clone RM4-4) AF700 (Biolegend) or CD4 605 (BD Bioscience), CD25 PEcy7 (BD Bioscience), LAP PerCP-eFluor710, CD44 PEcy5 or CD44 v450, CD62L PE-CF594 (BD Bioscience) or CD62L PerCP-cy5.5, NK1.1 AF700 and/or FasL PE (Biolegend). Samples from CD4 depleted mice were also stained separately for the inflammatory cell and lymphocyte cocktails (surface markers) described in the first paragraph above. Fixed samples were analyzed using the BD LSRFortessa or LSRII Flow Cytometer (BD Biosciences) as described above.

Data analysis was completed using FlowJo VX version (Tree Star Inc. USA). Gating of immune cell populations (as well as cytokine, granzyme B and FasL expression on cells) was performed based on the combination of antibody stains shown in Table S1 and Figure S7.

CD8 antibody depletion

C57BL/6J mice were depleted of CD8+ T cells as described (Kruisbeek, 2001). The neutralizing monoclonal antibody CD8 2.43 or IgG2b isotype control (Antibody Services, Walter and Eliza Hall Institute Biotechnology Centre, Melbourne) was injected intraperitoneally (0.1mg dose) in mice for three consecutive days (day 1-3) at 4 weeks after TBI in a blinded manner; the administrator was uninformed as to which mice received which treatment. Mice received two more weekly injections at day 8 and 15 to maintain depletion. Submandibular bleeding was performed on days 6 and 20 to determine the extent of depletion by flow cytometry. Blood samples of approximately 100μl volume were immersed with 8 mL of red blood cell (RBC) lysis buffer (156mM NH_4Cl, 11.9mM $NaHCO_3$ and 0.097mM EDTA) to remove RBCs. This step was repeated followed by centrifugation at 1500 rcf for 5 min. Samples were stained (50μl/sample) with the following fluorescent antibody markers; rat anti-mouse CD8b.2 APC (BioLegend Inc. USA), CD45 PE (BD, Australia), CD3 APC-eFluor780 (BD, Australia) and CD4 BV605 (BioLegend Inc. USA) as described above. Samples were resuspended in PBS with 2% FBS alone and then analyzed the same day using the BD LSRFortessa cell analyzer.

CD4 antibody depletion

C57BL/6J mice were depleted of CD4+ T cells starting at 1 week post-TBI. This time-point was selected as levels of CD4+ T cells are increased in the brain at this 1 week time-point (data not shown). Mice received either the neutralizing monoclonal antibody CD4 GK1.5 or IgG2b isotype control (Antibody Services, Walter and Eliza Hall Institute Biotechnology Centre, Melbourne) at a dose of 0.1mg following the protocol described above (CD8 antibody depletion), although beginning at 1 week post-TBI (i.e., three consecutive daily injections followed by five weekly injections thereafter). Following submandibular bleeding to determine extent of depletion at day 9 and 20, samples were stained (50μl/sample) with the following fluorescent antibody markers; rat anti-mouse CD8b.2 APC (BioLegend Inc. USA) or CD8a FITC, CD45 PE (BD, Australia), CD3 APC- eFluor780 (BD, Australia) and CD4 PerCP (BD, Australia) as described above and analyzed the same day using the BD LSRFortessa cell analyzer.

Blood collection

Blood was collected from the vena cava of euthanized mice using a 23-gauge syringe. Blood was allowed to clot at room temperature and serum was then obtained after centrifugation for 10 min at 9300 rcf. Alternatively, blood was collected in a syringe containing 10% anticoagulant 129mM sodium citrate (pH 7.4) and then centrifuged for 15 min at 3000 rcf for plasma collection. Serum/plasma samples were stored at −80°C until required for further analysis.

Detection of serum autoantibodies via ELISA

The presence of circulating autoantibodies against brain antigens (myelin and dsDNA) was investigated after TBI over the course of 32 weeks. Nunc MaxiSorp® flat-bottom 96 well plates (eBioscience Inc. USA) were coated (100μl) overnight at 4°C with 5μg/ml $PLP_{139-151}$ peptide or MOG_{35-55} peptide (GM Biochem (Shanghai) Ltd) in 0.05M carbonate-bicarbonate coating buffer (Bethyl Laboratories, USA). Blocking buffer (1% BSA/1x tris buffered saline (TBS) w/v) was then added for a further 90 min at room temperature, followed by washing with 1xTBS + 0.05% Tween-20 three times before use. For dsDNA ELISA, plates were coated (50 μl) with 1μg/ml of dsDNA (Sigma-Aldrich, USA) in 100 mM Tris-HCl (pH 8) and incubated overnight at 4°C in a humidified box. Plates were washed three times with 0.05% Tween-20/1xPBS and blocked with Assay Diluent (BD Biosciences, USA) for 1 h at room temperature and then washed again. Diluted serum or plasma (100 μl) was added to appropriate wells in duplicate (for each plate/antigen); control wells were incubated with diluent alone. Diluent used for MOG/PLP ELISA was 1% BSA (w/v) / 1x TBS/ 0.05% Tween-20. All plates were incubated for 2 h (or 4 h for plasma samples; MOG/PLP ELISA) at room temperature (in a humidified box for dsDNA ELISA) and washed with appropriate wash buffer four times. HRP conjugated goat anti-mouse IgG (Bethyl Laboratories, USA) was added and incubated for 1 h at room temperature. This secondary antibody was used at a 1:2000 (serum samples) or 1:1000 (plasma samples) dilution, prepared in diluent. After washing (3x), Tetramethylbenzidine (TMB) peroxidase substrate (Bethyl Laboratories, USA) was added (100μl) and the plates incubated in the dark for 30 min. Sulphuric acid (2M) was then added to each well to stop the reaction, and the optical density (OD_{450nm}) was determined with the FLUOstar OPTIMA Microplate Reader (BMG LABTECH Pty. Ltd. Australia). Data analysis involved calculating the average OD for the duplicates of each sample, which was subtracted by the average OD of the blank control wells (background).

Multiplex cytokine assay

Cytokine profiling of serum or plasma samples was performed using the *Bio-Plex Pro Mouse Cytokine 23-plex Assay* (Bio-Rad Laboratories Pty., Ltd. Australia) measured the following cytokines/chemokines; IL-1α, IL-1β, IL-2, IL-3, IL-4, IL-5, IL-6, IL-9, IL-10, IL-12 (p40), IL-12 (p70), IL-13, IL-17A, Eotaxin, G-CSF, GM-CSF, IFN-γ, KC, MCP-1, MIP-1α, MIP-1β, RANTES, TNF-α. Serum (WT and β2 $m^{-/-}$) or plasma (CD8+ T cell-depleted and μ-MT) samples were assayed at the 8 week time-point according to manufacturer's instructions then read on the Bio-Plex® 100 System (Bio-Rad Laboratories Pty., Ltd. Australia). Briefly, a 96 well 'flat-bottom' plate was coated (50μl/well) with diluted magnetic beads (1:10 dilution of supplied 10x coupled beads). Plates were washed twice with Bio-Plex wash buffer using the handheld magnetic washer (Bio-Rad Laboratories). Diluted samples (1:4) or standards (1.95 pg/ml to 32,000 pg/ml) were added (50μl) to appropriate wells and blank controls contained diluent only. The plate was incubated in the dark for 30 min at room temperature on a plate shaker (850 ± 50 rpm). After washing with Bio-Plex wash buffer (3x) as above, diluted detection antibodies were added to each well (25μl) and incubated for 30 min at room temperature on a plate shaker (850 ± 50 rpm). Following another set of washes (3x), diluted streptavidin-PE was then added and incubated on a plate shaker for 10 min at room temperature. After a final three sets of washing plates, samples were resuspended in Bio-Plex assay buffer and placed on plate shaker for 30 s immediately before the plate was analyzed. The plate was read using the Bio-Plex 100 system (Bio-Rad) on the low RP1 (PMT) settings as recommended. The Bio-Plex Manager Software was used to determine the median fluorescence intensity (MFI) of each sample, and the concentration (pg/ml) of each cytokine/chemokine was then identified in samples using the standard curve.

Histology and microscopy imaging

Haematoxylin and eosin (H&E) and Luxol Fast Blue (LFB) staining of paraffin embedded brain tissue sections (8μm; prepared using the Leica RM2165 microtome (Leica Microsystems Pty Ltd Australia) were undertaken by the Monash Histology Platform, Melbourne according to standard protocols as briefly described below. For H&E staining, slides were deparaffinised by multiple immersions in xylene followed by absolute ethanol (100%) and then low-grade ethanol (70%). Slides were rinsed with water before being submerged in Mayer's Haematoxylin solution and then Eosin solution (counterstain), with water rinses and differentiation (1% acid

alcohol) in between staining. Sections were dehydrated with multiple stages of low to high grade ethanol immersions. Slides were cleared by submersion in xylene, mounted with coverslips and allowed to dry at room temperature. For LFB staining, slides were initially deparaffinised with xylene and hydrated with multiple immersions in absolute ethanol. Slides were submerged in LFB solution and incubated overnight in a 60°C oven. The following day, sections were rinsed in high-grade ethanol (95%) and dH_2O before being differentiated with 0.05% lithium carbonate solution and then in low-grade ethanol (70%), followed by rinsing with dH_20. The differentiation steps were repeated until there was contrast between white matter and gray matter. Sections were counterstained with cresyl violet, washed with dH_2O and then submerged in absolute ethanol multiple times. Finally, slides were cleared with xylene, mounted with coverslips and allowed to dry at room temperature.

For lymphocyte detection (CD8) by DAB immunostaining, sections were first dewaxed with xylene (3x 5 min), dehydrated with 100% ethanol and washed with PBS. Antigen retrieval using 10mM sodium citrate was then performed for 20 min, in a 90°C water bath, and a further 30 min at room temperature. After washing with PBS (3x), slides were incubated with 1% hydrogen peroxide for 5 min, permeabilised with 0.5% Triton-X and blocked with 10% horse serum for 1 h in a humidified chamber. Rat anti-mouse CD8 antibody (1:50, 4SM16 clone, Thermo Fisher Scientific, Australia) was incubated overnight in a humidified chamber at 4°C. After washing again with PBS (3x), biotinylated rabbit anti-rat IgG (Vector Laboratories) was incubated (1:200) for 1 h in a humidified chamber. After washing with PBS (3x), samples were incubated for 30 min with VECTASTAIN Elite avidin-biotin complex (ABC)-HRP kit solution (Vector Laboratories) and then developed using ImmPACT DAB substrate kit (Vector Laboratories) for 10 min. All sections were counterstained with Mayer's Haematoxylin for 2 min, rinsed with dH_2O, cleared with ethanol and xylene, and then coverslipped using DPX mounting medium.

Bright-field images at x4, x10, x40 or x100 magnification (i.e., H&E and LFB, and CD8 immunostaining) were captured using the Olympus BX51 microscope fitted with a digital camera (Olympus DP70; Olympus Australia Pty Ltd). Sections from all cohorts were batch-stained to minimize variability in staining intensity, allowing for accurate comparisons to be made. Camera settings were consistent between the different sections and images were analyzed using the ImageJ software, version 1.50i (NIH, USA).

QUANTIFICATION AND STATISTICAL ANALYSIS

Statistical analysis

Data are expressed as mean ± SEM. The Student's t test (unpaired, two-tailed) was performed to determine statistical significance between TBI and sham controls (or CD8/ CD4 depleted and IgG controls) at each time-point for flow cytometry, LFB quantitation and multiplex cytokine analysis. One-way ANOVA test with Newman Keuls post hoc test was used for assessing flow cytometry data containing three groups (TBI, sham and sham NC) and for the probe trial for Morris water maze (IgG control and CD4 depleted or CD8 depleted). The two-way repeated-measures ANOVA test with Bonferroni post hoc test was used to statistically assess neurological outcome over 32 weeks. To evaluate changes in motor function over this period, a two-way ANOVA with Fisher's LSD post hoc test was carried out to compare injured and sham animals for gait parameters measured. Two-way ANOVA with Bonferroni's post hoc test was conducted as a statistical measure of injured and sham controls for ELISA experiments. Two-way repeated-measures ANOVA with Newman Keuls post hoc test was used for Morris water maze analysis. A two-way ANOVA with Newman Keuls post hoc test was corrected for multiple comparisons for Th17-related cytokine analysis. P values of less than 0.05 were deemed significant using GraphPad Prism (version 6.01; GraphPad Software Inc. USA). The distribution of the data were determined to follow either a normal or lognormal distribution (i.e., passed normality tests) using GraphPad Prism and the appropriate statistical tests were then used. Outlier tests were performed when appropriate using this software (e.g., ROUT/Grubbs outlier test). Statistical details including statistical tests used, n value (number of animals = biological replicates), precision measures (SEM) and p values can be found in the corresponding figure legends for individual experiments.

Quantification of myelin vacuolisation in spinal cord sections

LFB stained spinal cord sections were quantitated for demyelination/vacuolisation using ImageJ software, version 1.50i (NIH, USA), by determining the percentage of the white area (i.e., vacuoles) over the total area of each section. One brain or spinal cord section from three to six mice per cohort (n = 3-6 biological replicates) were studied.

DATA AND CODE AVAILABILITY

This study did not generate any unique datasets or code.